RESTRICTED
LANGLEY SUB-LIBRARY
UNAVAILABLE
NACA
CLASSIFICATION CANCELLED
OCT 15 1946

RM E6I24

Title Unavailable by Admin. Action per Hdqrs. ltr. dtd. 6-8-59 BAM.

RESEARCH MEMORANDUM

for the

Air Materiel Command, Army Air Forces

ALTITUDE-WIND-TUNNEL INVESTIGATION OF PERFORMANCE OF SEVERAL PROPELLERS ON YP-47M AIRPLANE AT HIGH BLADE LOADING

I - AEROPRODUCTS H20C-162-X11M2 FOUR-BLADE PROPELLER

By Martin J. Saari and Lewis E. Wallner

Aircraft Engine Research Laboratory
Cleveland, Ohio

FOR REFERENCE

NOT TO BE TAKEN FROM THIS ROOM

CONTAINS PROPRIETARY INFORMATION

CLASSIFIED DOCUMENT

This document contains classified information affecting the National Defense of the United States within the meaning of the Espionage Act, USC 50:31 and 32. Its transmission or the revelation of its contents in any manner to an unauthorized person is prohibited by law. Information so classified may be imparted only to persons in the military and naval Services of the United States, appropriate civilian officers and employees of the Federal Government who have a legitimate interest therein, and to United States citizens of known loyalty and discretion who of necessity must be informed thereof.

NATIONAL ADVISORY COMMITTEE FOR AERONAUTICS

WASHINGTON

OCT 11 1946

UNAVAILABLE
NACA LIBRARY
LANGLEY MEMORIAL AERONAUTICAL LABORATORY
Langley Field, Va.

RESTRICTED

NASA Technical Library
3 1176 01435 0285

UNAVAILABLE

NACA RM No. E6I24

NATIONAL ADVISORY COMMITTEE FOR AERONAUTICS

RESEARCH MEMORANDUM

for the

Air Materiel Command, Army Air Forces

ALTITUDE-WIND-TUNNEL INVESTIGATION OF PERFORMANCE OF SEVERAL PROPELLERS ON YP-47M AIRPLANE AT HIGH BLADE LOADING

I - AEROPRODUCTS H20C-162-X11M2 FOUR-BLADE PROPELLER

By Martin J. Saari and Lewis E. Wallner

SUMMARY

An investigation was made in the Cleveland Altitude wind tunnel to determine the performance of an Aeroproducts H20C-162-X11M2 four-blade propeller on a YP-47M airplane at high blade loadings and high engine powers. The propeller characteristics were obtained for a range of power coefficients from 0.30 to 1.00 at free-stream Mach numbers of 0.40 and 0.50. The results of the force measurements are indicative only of trends in propeller efficiency with changes in power coefficient and advance-diameter ratio because unknown interference effects existed during the investigation.

At a free-stream Mach number of 0.40, the envelope of the efficiency curves decreased about 8 percent between advance-diameter ratios of 1.80 and 4.20. Nearly constant maximum efficiencies were obtained at power coefficients from 0.30 to 0.60 for advance-diameter ratios from 1.70 to 2.40. The advance-diameter ratio for peak efficiency increased as the power coefficient was increased. For advance-diameter ratios below 2.90 the propeller efficiency decreased rapidly at power coefficients above 0.60 apparently caused by blade stall. In the range of advance-diameter ratios above 2.90, the propeller efficiency improved as the power coefficient increased.

At a free-stream Mach number of 0.50, the envelope of the efficiency curves decreased about 11 percent between advance-diameter ratios of 2.40 and 4.40. An increase in power coefficient from 0.30 to 0.80 at an advance-diameter ratio of 2.40 had little effect on the propeller efficiency. A change in power coefficient from 0.40 to 1.00 at an advance-diameter ratio of 4.40 increased the propeller efficiency by about 40 percent.

UNAVAILABLE

RESTRICTED

For conditions below the stall the thrust loading on the outboard blade sections increased more rapidly than on the inboard sections as the power coefficient was increased or as the advance-diameter ratio was decreased. For conditions beyond the stall the thrust loading decreased on the outboard sections and increased on the inboard sections.

INTRODUCTION

Propeller investigations conducted in NACA wind tunnels at high blade loadings (power coefficients up to 1.8), low airspeeds, low engine powers and low propeller rotational speeds are reported in references 1 to 3. Other studies made in flight at high airspeeds, engine powers and engine speeds but at relatively low power coefficients (up to 0.40) are reported in references 4 to 7. Developments in aircraft power plants providing high powers at high altitudes make necessary the investigation of propeller performance at high power coefficients, engine powers, propeller rotational speeds and relatively high airspeeds.

An investigation of the performance characteristics of several propellers on the YP-47M airplane at high blade loadings has been conducted in the Cleveland altitude wind tunnel at the request of the Air Materiel Command, Army Air Forces. As part of this investigation the efficiencies and blade thrust load distributions were determined for the Aeroproducts H20C-162-X11M2 four-blade propeller over a wide range of operating conditions. Similar data are being obtained on other propellers.

The range of power coefficients covered was from 0.30 to 1.00 at free-stream Mach numbers of 0.40 and 0.50. The engine combustion air was supplied to the turbosupercharger at sea-level conditions and the propeller was operated at density altitudes from 20,000 to 45,000 feet. Engine powers ranged from 150 to 2000 brake horsepower and engine speeds from 1100 to 2900 rpm. The blade thrust load distribution was obtained from two diametrically opposed slipstream survey rakes.

PROPELLER AND POWER PLANT

A description of the propeller and power plant is as follows:

Propeller	
Hub	A642F-X17
Blade design	Aeroproducts H20C-162-X11M2
Number of blades	four
Blade sections	NACA 16 series
Propeller diameter	12 feet 7 inches
Activity factor[1]	107
Propeller gear ratio	20:9
Engine	R-2800-73
War emergency power rating:	
Engine speed, rpm	2800
Manifold pressure, in. Hg	72.0
Brake horsepower	2800
Military power rating:	
Engine speed, rpm	2800
Manifold pressure, in. Hg	53.5
Brake horsepower	2100
Normal power rating:	
Engine speed, rpm	2600
Manifold pressure, in. Hg	41.5
Brake horsepower	1700

[1]The activity factor is a nondimensional function of the propeller plan form designed to express the integrated capacity of the propeller blade elements for absorbing power (reference 8) and is expressed as

$$A.F. = \frac{100,000}{16} \int_{0.2}^{1.0} \frac{b}{D} \left(\frac{r}{R}\right)^3 d\left(\frac{r}{R}\right)$$

where

b blade width at radius r

D propeller diameter

R propeller radius to tip

r radius of any blade element

The propeller blade-form characteristics are given in figure 1. A photograph of an Aeroproducts H20C-162-X11M2 propeller blade is shown in figure 2.

APPARATUS

A fuselage of a YP-47M airplane with stub wings was installed in the 20-foot-diameter test section of the wind tunnel with the thrust axis of the airplane parallel to and about 12 inches above the axis of the test section. The Aeroproducts H20C-162-X11M2 propeller and the R-2800-73 engine were incorporated in the airplane as shown in figure 3. The engine was provided with refrigerated combustion air at sea-level pressure from an external source by a duct passing through the left wing stub and the fuselage to the inlet of the turbosupercharger. The combustion-air temperature was maintained at approximately 10° F.

Pressure and temperature surveys were made at all cooling-air inlets and outlets and exhaust-gas outlets to determine the internal momentum losses and exhaust-jet thrust. Pressures were measured by water manometers and were photographically recorded. The temperatures were recorded by self-balancing potentiometers.

Engine horsepower was measured within ±2 percent by a calibrated Pratt & Whitney torquemeter and a pressure gage. Propulsive thrust was measured and recorded by the tunnel drag balance, which measures the resultant force on the airplane in the direction of the thrust axis.

A survey was conducted of the total pressure in the propeller slipstream by two rakes, each consisting of 32 shielded total-head tubes $2\frac{1}{2}$ inches apart, one on each side of the airplane 46 inches behind the propeller disk as shown in figure 4. The rakes were attached to the tunnel wall in the horizontal plane of the thrust axis and extended to within three-fourths inch of the engine cowling.

PROCEDURE

The readings of temperature, pressure, horsepower, and the resultant thrust force were obtained for a range of power coefficients from 0.30 to 1.00 at free-stream Mach numbers of 0.40 and 0.50. Density altitudes from 20,000 to 45,000 feet were simulated for engine powers from 150 to 2000 brake horsepower at engine speeds from 1100 to 2900 rpm. Runs were made with the propeller removed at the beginning and the end of the program for ranges of tunnel airspeeds, density altitudes, and cowl flap deflections.

REDUCTION OF DATA

The external drag D_e of the installation was evaluated as the difference between the total drag D and the internal cooling-air momentum losses D_i obtained from runs with the propeller removed. The external-drag values obtained at the end of the program were as much as 9 percent greater than the values obtained at the beginning of the program. The increase is attributed to the deterioration of the installation by distortion of surfaces and accumulation of dirt on the surfaces of the airplane. An average of the two drag coefficients was used in calculation of external drag.

An attempt was made to correct the installation drag for differences in horizontal buoyancy between propeller-removed and propeller-operating conditions by the methods given in references 9 and 10 but the results were too inconsistent to be reliable and were therefore not applied. No effort was made to correct the installation drag for the effects of the propeller slipstream. The change in free-stream velocity in the plane of the propeller disk resulting from inflow, tunnel-wall constriction and proximity of the airplane cowling was not determined.

The propeller thrust T was determined by

$$T = T_p + D_e + D_i - T_j$$

where

T_p propulsive thrust read on drag scale, pounds

T_j jet thrust of exhaust gases, calculated from pressure and temperature surveys in exhaust-gas outlets, pounds

The value of T as defined is an approximate value because corrections for tunnel-wall constriction were not applied.

The thrust coefficient C_T was calculated from

$$C_T = \frac{T}{\rho n^2 D^4}$$

where

ρ free-stream density, slugs per cubic foot

n propeller rotational speed, revolutions per second

D propeller diameter, feet

The power coefficient C_P was calculated from

$$C_P = \frac{P}{\rho n^3 D^5}$$

where P is the engine power in foot pounds per second. The propeller efficiency η was computed from

$$\eta = \left(\frac{C_T}{C_P}\right) J$$

where J is the advance-diameter ratio V/nD, V being the tunnel free-stream velocity.

The propeller tip Mach number M_t was calculated from

$$M_t = M_o \sqrt{1 + \left(\frac{\pi}{J}\right)^2}$$

where M_o is the free-stream Mach number.

Propeller efficiencies were also determined by the slipstream survey method described in references 3 and 5 but the results were inconsistent with the values obtained from force measurements. The surveys are of value, however, in showing the blade thrust load distribution for various operating conditions. The blade thrust loading is presented as the rise in total-head pressure $H_s - H_o$ across the propeller disk where H_s is the total pressure measured by the slipstream survey rake and H_o is the free-stream total pressure.

The results of the force measurements indicate primarily the trend of propeller efficiency with changes in power coefficient and and advance-diameter ratio because corrections for tunnel-wall constriction effects on the installation were not applied.

RESULTS AND DISCUSSION

The propeller characteristics for various blade loading conditions are presented separately for free-stream Mach numbers of 0.40 and 0.50 because it is not possible to compare the data obtained at different free-stream Mach numbers. Slipstream surveys are presented to illustrate blade thrust load distribution in terms of the total-pressure rise across the propeller disk for certain operating conditions.

Free-stream Mach number, 0.40. - The variation of propeller efficiency η with advance-diameter ratio J for values of power coefficient C_p from 0.30 to 1.00 at a free-stream Mach number of 0.40 is shown in figure 5. The variation of propeller efficiency with power coefficient is shown in figure 6 for three approximately constant values of advance-diameter ratio. The dashed curves were cross-plotted from an extrapolation of figure 5.

The effect of increasing the power coefficient from 0.30 to 1.00 was to reduce the propeller efficiency at low advance-diameter ratios and to increase the efficiency at high advance-diameter ratios. The envelope of the efficiency curves decreased about 8 percent between advance-diameter ratios of 1.80 and 4.20. In the range of advance-diameter ratio from 1.70 to 2.40, maximum efficiencies were obtained at power coefficients from 0.30 to 0.60. (See fig. 5.) The advance-diameter ratio for peak efficiency increased with power coefficient. Serious losses in propeller efficiency became evident at values of advance-diameter ratios from 1.70 to 2.90 for values of power coefficients above 0.60. (See figs. 5 and 6.) These losses may be attributed to blade stall caused by high operating angle of attack and by the probable reduction of the maximum section lift coefficient associated with high operating tip Mach numbers. (See references 11 and 12.) In order to illustrate the magnitude of these losses in efficiency, a change in power coefficient from 0.60 to 0.70 at an advance-diameter ratio of 1.75 resulted in a 20-percent reduction in efficiency. A further change in power coefficient from 0.70 to 0.90 reduced the efficiency an additional 20 percent. For values of advance-diameter ratio above 2.90 the propeller efficiency increased as the power coefficient was increased from 0.30 to 0.80 (figs. 5 and 6).

The effect of power coefficient on blade thrust load distribution is shown by the slipstream surveys in figure 7, which correspond to the conditions of figure 6 for an advance-diameter ratio of 1.75. The blade thrust load distributions for power coefficients from 0.30 to 0.59 were uniform and similar except that as the power coefficient was increased the loading on the outboard sections increased more rapidly than on the inboard sections. (See figs. 7(a) to 7(d).) When the power coefficient was changed from 0.59 to 0.69, blade stall, indicated by a reduction in total-pressure rise, occurred on the outboard sections, which caused the loading on the inboard sections to increase (fig. 7(e)). The increased loading on the inboard sections apparently originates from tip stall. At constant power operation, stalling of the propeller-blade tips creates a torque unbalance for which the propeller compensates by an increase in blade angle. The increased blade angle causes additional sections inboard of the tips to stall

and the stall region progresses gradually inboard until a state of torque equilibrium is reached. Because of the blade angle increase, the unstalled inboard sections operate at high lift coefficients and consequently the thrust loading is high. At values of power coefficient of 0.78 and 0.90 the region of stall extended inboard as far as $(r_s/R)^2 = 0.40$ or more than 35 percent of the blade span. (See figs. 7(f) and 7(g).)

The difference between the right-side and left-side surveys was apparently due to an upward inclination of the approaching air stream to the propeller axis caused by the lift of the wing. The right, or downgoing, blades therefore operated at higher angles of attack than the left, or upgoing, blades and thus produced more thrust. For the same reasons, the right blades stalled earlier and the losses due to stall were slightly greater than for the left blades. This phenomenon is explained in greater detail in references 6 and 13.

The development of blade stall for power coefficients of 0.70 and 0.90 is shown in figures 8 and 9, respectively. For a power coefficient of 0.70 and an advance-diameter ratio of 4.00, the thrust loading over the blades was very low especially at the tip sections (fig. 8(a)). At a constant C_p, a reduction in J resulted in an increase of angle of attack and section lift coefficients; the thrust loading increased steadily up to the stall point. (See figs. 8(b) and 8(c).) Blade stall was evident at an advance-diameter ratio of 1.73 and at an advance-diameter ratio of 1.58 the stall, further aggravated by increased angle of attack and tip Mach number, extended to sections as far inboard as $(r_s/R)^2 = 0.40$ (fig. 8(e)). The survey shown in figure 8(e) illustrates, as previously discussed, that the right-side blades stall first and the losses in thrust are slightly greater than on the left-side blades. The stall developed in a similar manner for a power coefficient of 0.90 except that it occurred at a somewhat higher advance-diameter ratio owing to the greater required blade angle. The initial stall apparently occurred at an advance-diameter ratio between 2.94 and 2.07 because at 2.07 the stall was in an advanced stage. (See figs. 9(a) and 9(b).) A further reduction in advance-diameter ratio resulted in stalling of all sections outboard of $(r_s/R)^2 = 0.40$ (figs. 9(c) and 9(d)).

Free-stream Mach number, 0.50. - The variation of propeller efficiency with advance-diameter ratio for power coefficients from 0.30 to 1.00 at a free-stream Mach number of 0.50 is presented in figure 10. The variation of propeller efficiency with power coefficient at approximately constant values of advance-diameter ratio is shown in figure 11.

The envelope of the efficiency curves decreased about 11 percent between advance-diameter ratios of 2.40 and 4.40. An increase in power coefficient from 0.30 to 0.80 at an advance-diameter ratio of approximately 2.40 had little effect on the propeller efficiency and nearly constant maximum efficiencies were obtained. (See fig. 10.) As the advance-diameter ratio was increased from 2.40 to 4.40 the effect of increasing the power coefficient became more pronounced. A change in power coefficient from 0.40 to 1.00 at an advance-diameter ratio of 4.40 increased the propeller efficiency by about 40 percent. (See figs. 10 and 11.)

The effect of power coefficient on blade thrust load distribution is shown by the slipstream surveys in figure 12, which correspond to conditions of figure 11 for an advance-diameter ratio of about 2.80. A change in power coefficient from 0.30 to 0.83 resulted in a uniform increase in thrust loading over the blade span. There were no significant irregularities in the thrust load distribution curves that would indicate blade stall at any power coefficient. Similar surveys are presented in figure 13 for a range of power coefficients from 0.42 to 0.93 at an advance-diameter ratio of approximately 4.40. At a power coefficient of 0.42 the thrust loading was very low particularly on the outboard sections (fig. 13(a)). As the power coefficient was increased to 0.93, the thrust loading on the inboard sections remained nearly constant and the loading on the outboard sections increased (figs. 13(b) to 13(d)). The surveys indicate that the thrust loading at high advance-diameter ratios could be considerably increased before adverse effects due to stall would be encountered.

Slipstream surveys for power coefficients of 0.70, 0.90, and 1.00 are presented in figures 14 to 16, respectively, for a range of advance-diameter ratios. In general, as the advance-diameter ratio was reduced at a given power coefficient the thrust loading on the outboard sections increased more rapidly than on the inboard sections. Within the range of advance-diameter ratios investigated, there was no evidence of blade stall for the power coefficients obtained.

A comparison of figures 14(b) and 8(b) shows that the thrust load distribution curves are similar for conditions run at approximately the same power coefficient and advance-diameter ratio but different tip Mach numbers. A similar comparison of figures 15(b) and 9(a) further indicates that below the stall a moderate increase in tip Mach number had little effect on blade thrust load distribution.

SUMMARY OF RESULTS

Corrections for the effects of tunnel-wall constriction on propeller characteristic parameters and on the installation have not been applied and the propeller efficiencies therefore only serve to show the comparative effects of blade loading on propeller performance. The investigation in the altitude wind tunnel of the performance at high blade loadings of an Aeroproducts H20C-162-X11M2 four-blade propeller on a YP-47M airplane indicated:

1. At a free-stream Mach number of 0.40, the envelope of the efficiency curves decreased about 8 percent between advance-diameter ratios of 1.80 and 4.20. Nearly constant maximum efficiencies were obtained for power coefficients from 0.30 to 0.60 at advance-diameter ratios from 1.70 to 2.40. The advance-diameter ratio for peak efficiency increased as the power coefficient was increased. In the low range of advance-diameter ratios (1.70 to 2.90), losses in propeller efficiency resulting from blade stall occurred at power coefficients above 0.60; an increase in power coefficient from 0.60 to 0.70 reduced the efficiency as much as 20 percent. For advance-diameter ratios above 2.90, the propeller efficiency increased as the power coefficient was increased from 0.30 to 0.80.

2. At a free-stream Mach number of 0.50, the envelope of the efficiency curves decreased about 11 percent between advance-diameter ratios of 2.40 and 4.40. An increase in power coefficient from 0.30 to 0.80 at an advance-diameter ratio of 2.40 has little effect on the propeller efficiency. A change in power coefficient from 0.40 to 1.00 at an advance-diameter ratio of 4.40 increased the efficiency by about 40 percent.

3. For conditions below the stall the thrust loading on the outboard blade sections increased more rapidly than on the inboard

sections as the power coefficient was increased or as the advance-diameter ratio was decreased. For conditions beyond the stall the thrust loading decreased on the outboard sections and increased on the inboard sections.

Aircraft Engine Research Laboratory,
National Advisory Committee for Aeronautics,
Cleveland, Ohio.

Martin J. Saari,
Aeronautical Engineer.

Lewis E. Wallner,
Mechanical Engineer.

Approved:

Alfred W. Young,
Mechanical Engineer.

Abe Silverstein,
Aeronautical Engineer.

lrp

REFERENCES

1. Biermann, David, Hartman, Edwin P., and Pepper, Edward: Full-Scale Tests of Several Propellers Equipped with Spinners, Cuffs, Airfoil and Round Shanks, and NACA 16-Series Sections. NACA ACR, Oct. 1940.

2. Biermann, David, and Hartman, Edwin P.: Wind-Tunnel Tests of Four- and Six-Blade Single- and Dual-Rotating Tractor Propellers. NACA Rep. No. 747, 1942.

3. McHugh, James G., and Pepper, Edward: The Characteristics of Two Model Six-Blade Counterrotating Pusher Propellers of Conventional and Improved Aerodynamic Design. NACA ARR, June 1942.

4. Vogeley, A. W.: Climb and High-Speed Tests of a Hamilton Standard No. 6507A-2 Four-Blade Propeller on the Republic P-47C Airplane. NACA MR No. L4K04, Army Air Forces, 1944.

5. Gardner, John J.: Effect of Blade Loading on the Climb and High-Speed Performance of a Three-Blade Hamilton Standard No. 6507A-2 Propeller on a Republic P-47D Airplane. NACA MR No. L5G09a, Army Air Forces, 1945.

6. Vogeley, A. W.: Climb and High-Speed Tests of a Curtiss No. 714-1C2-12 Four-Blade Propeller on the Republic P-47C Airplane. NACA ACR No. L4L07, 1944.

7. Vogeley, A. W.: Flight Measurements of Compressibility Effects on a Three-Blade Thin Clark Y Propeller Operating at Constant Advance-Diameter Ratio and Blade Angle. NACA ACR No. 3G12, 1943.

8. Dernbach, A. F.: Propeller Performance Calculation Procedure as Used by Propeller Laboratory. Memo. Rep. Ser. No. ENG-52-587-16-3, Materiel Command, Eng. Div., Army Air Forces, July 3, 1943.

9. Swanson, Robert S., and Gillis, Clarence L.: Wind-Tunnel Calibration and Correction Procedures for Three-Dimensional Models. NACA ARR No. L4E31, 1944.

10. Glauert, H.: Wind Tunnel Interference on Wings, Bodies and Airscrews. R. & M. No. 1566, British A.R.C., 1933.

11. Cleary, Harold E.: Effects of Compressibility on Maximum Lift Coefficients for Six Propeller Airfoils. NACA ACR No. L4L21a, 1945.

12. Spreiter, John R., and Steffen, Paul J.: Effect of Mach and Reynolds Numbers on Maximum Lift Coefficient. NACA TN No. 1044, 1946.

13. Pendley, Robert E.: Effect of Propeller-Axis Angle of Attack on Thrust Distribution over the Propeller Disk in Relation to Wake-Survey Measurement of Thrust. NACA ARR No. L5J02b, 1945.

INDEX OF FIGURES

Page

Page

Page

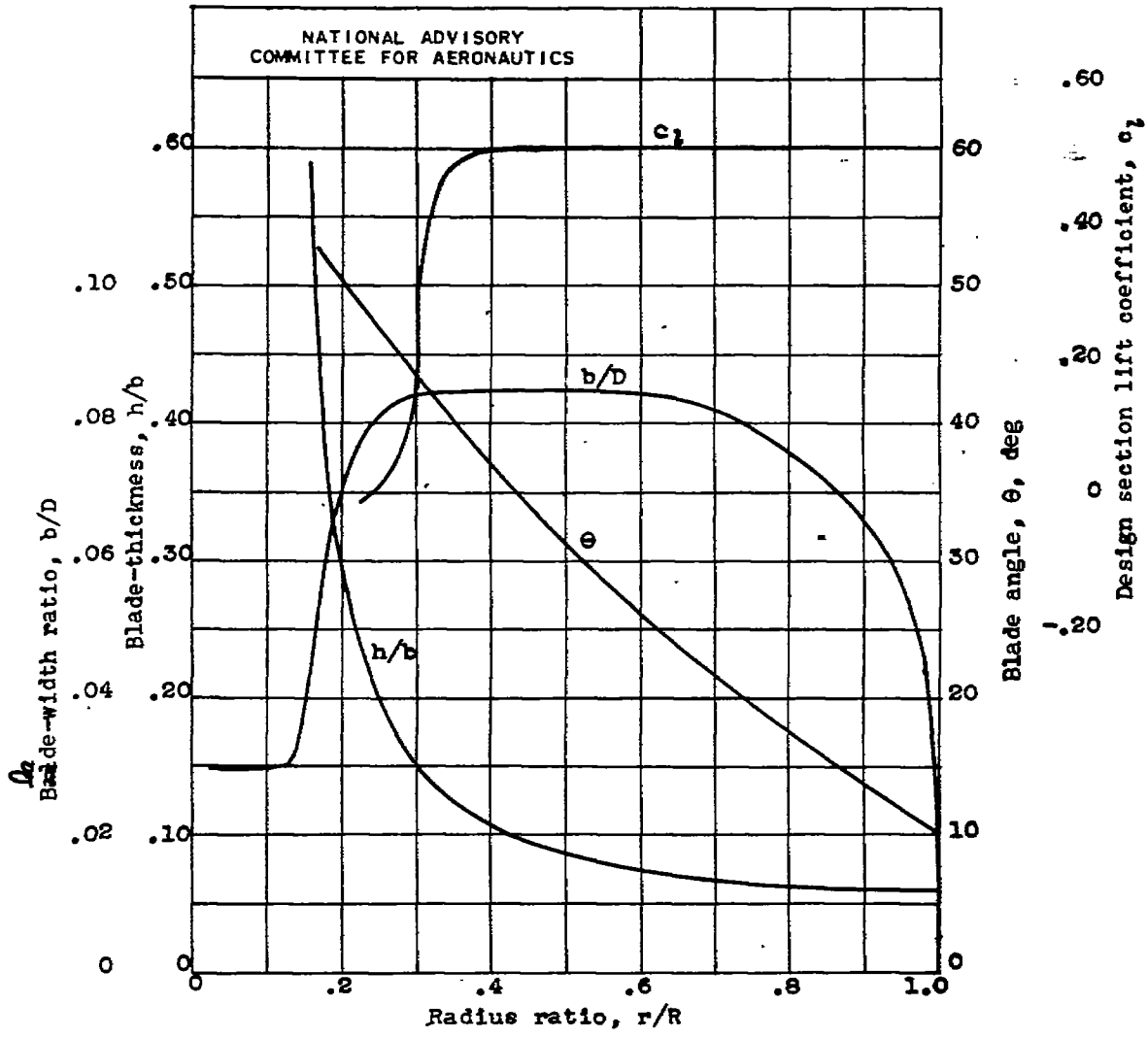

Figure 1.- Blade-form curves for Aeroproducts H20C-162-X11M2 four-blade propeller. b, section chord; D, diameter; h, section thickness; R, radius to tip; r, section radius.

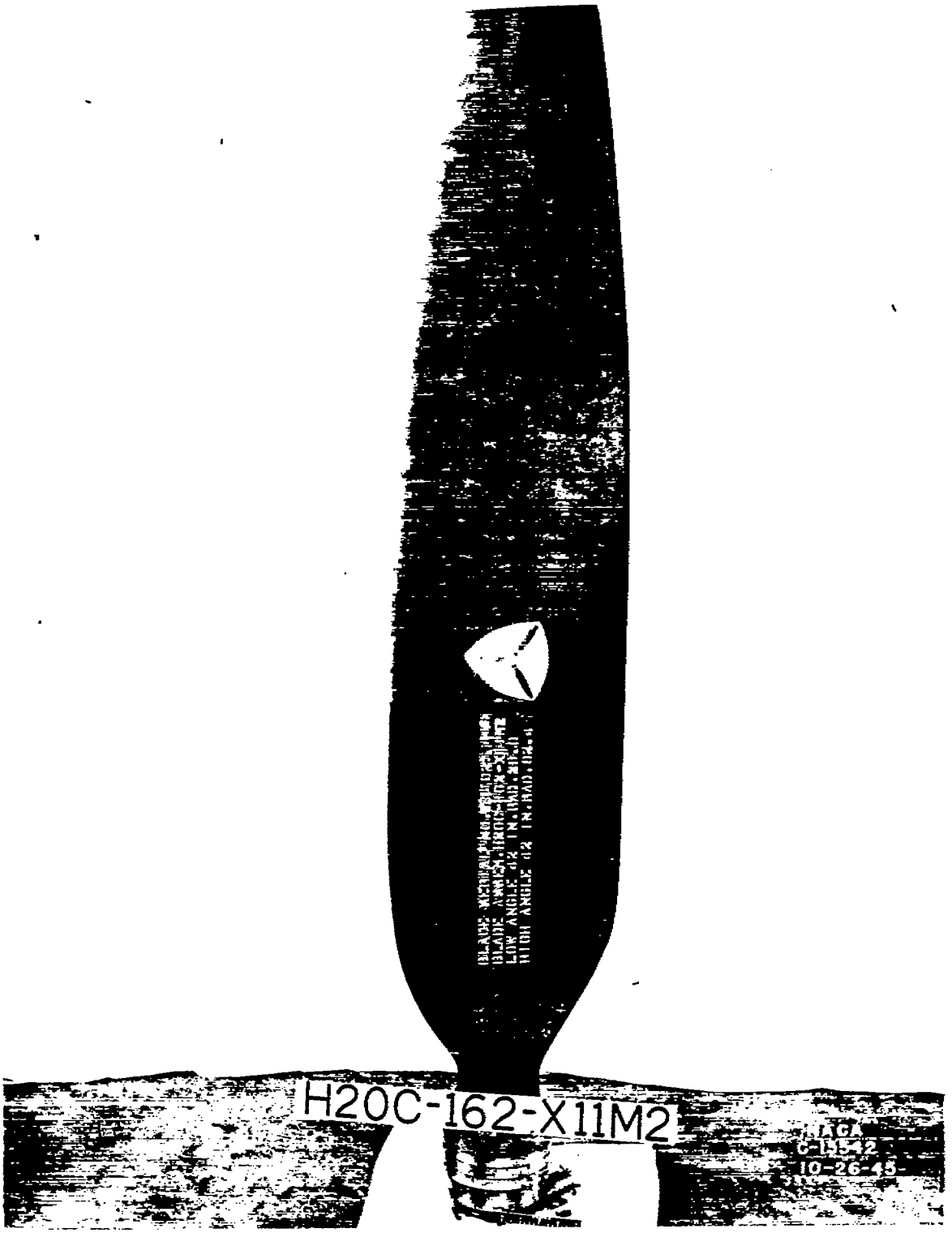

Figure 2. - Aeroproducts H20C-162-X11M2 propeller blade.

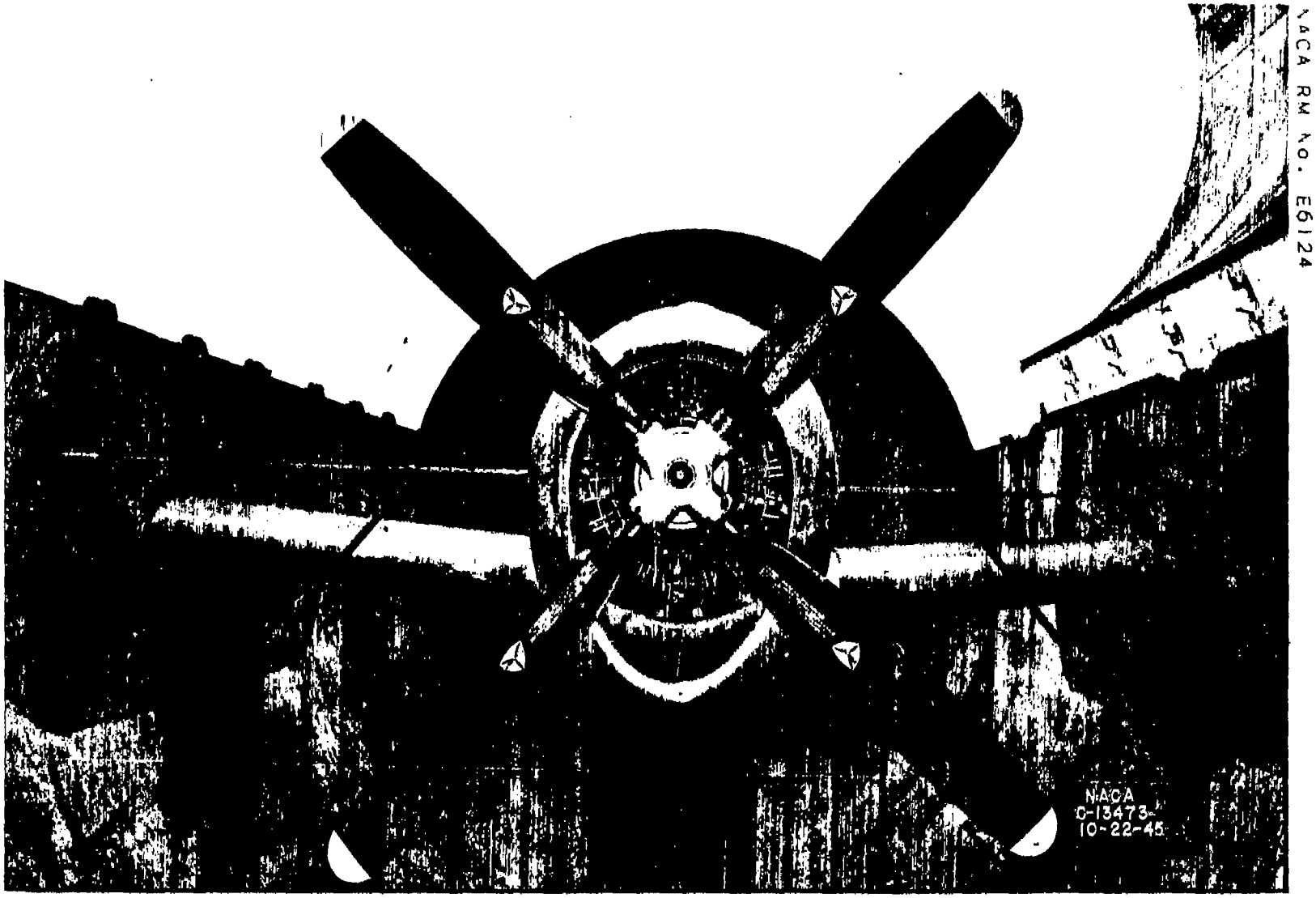

Figure 3. - Front view of YP-47M airplane with Aeroproducts [illegible] four-blade propeller installed in test section of altitude wind tunnel.

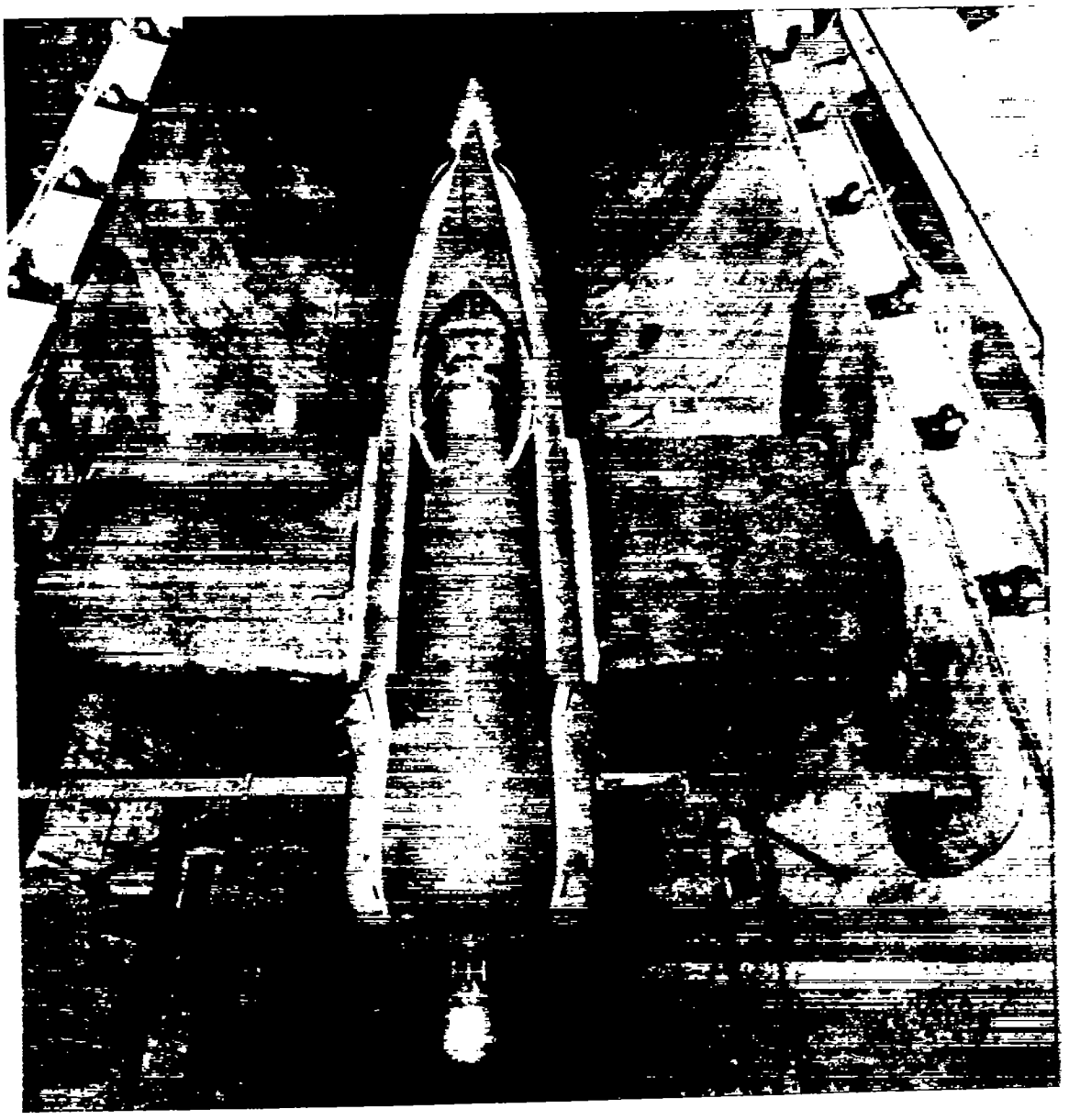

Figure 4. - Top view of YP-47M airplane in test section of altitude wind tunnel showing propeller-slipstream survey rakes.

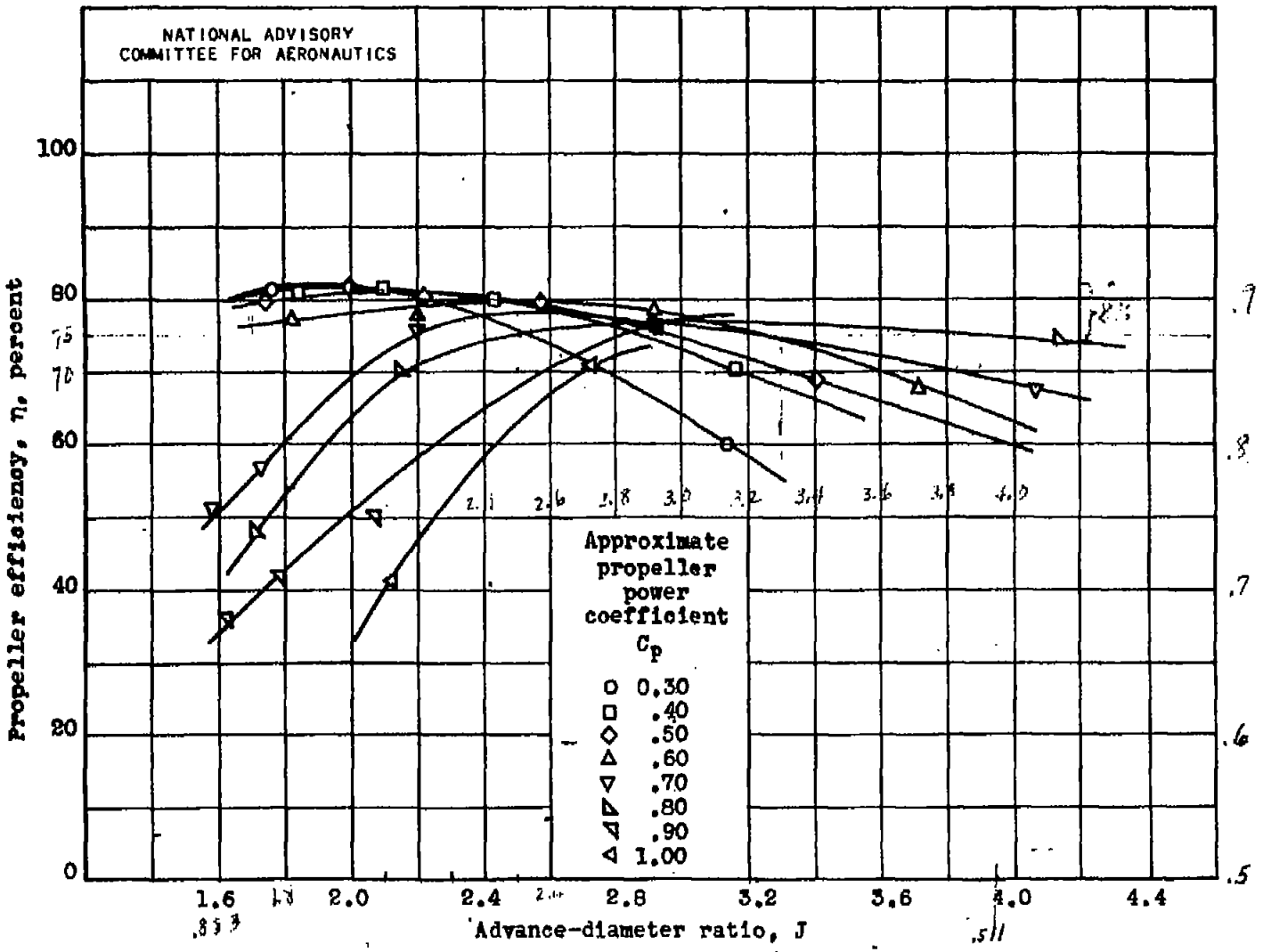

Figure 5.- Characteristics of Aeroproducts H20C-162-X11M2 four-blade propeller on YP-47M airplane at approximate free-stream Mach number M_o of 0.40.

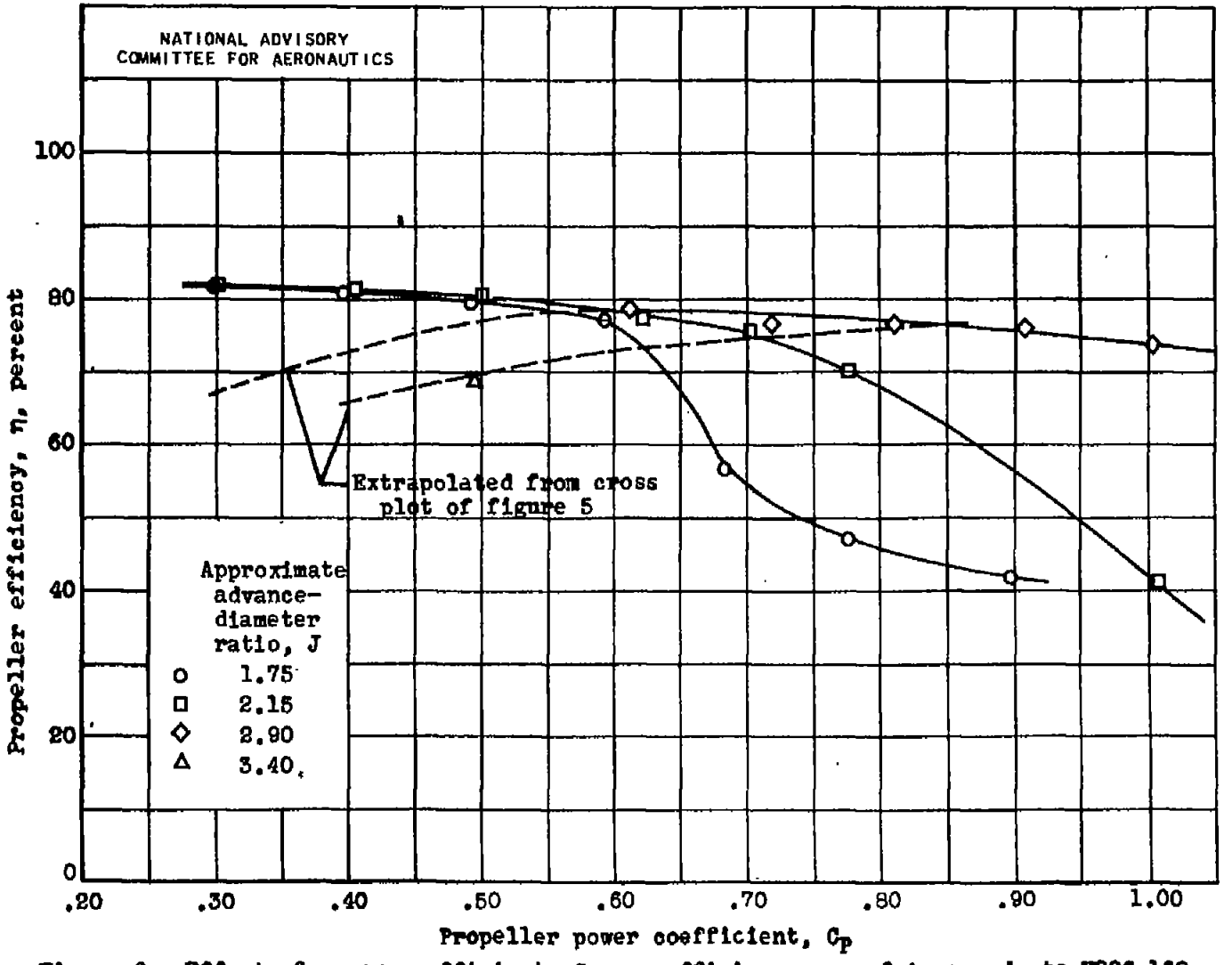

Figure 6.- Effect of power coefficient C_p on efficiency η of Aeroproducts H20C-162-X11M2 four-blade propeller at approximate free-stream Mach number M_o of 0.40.

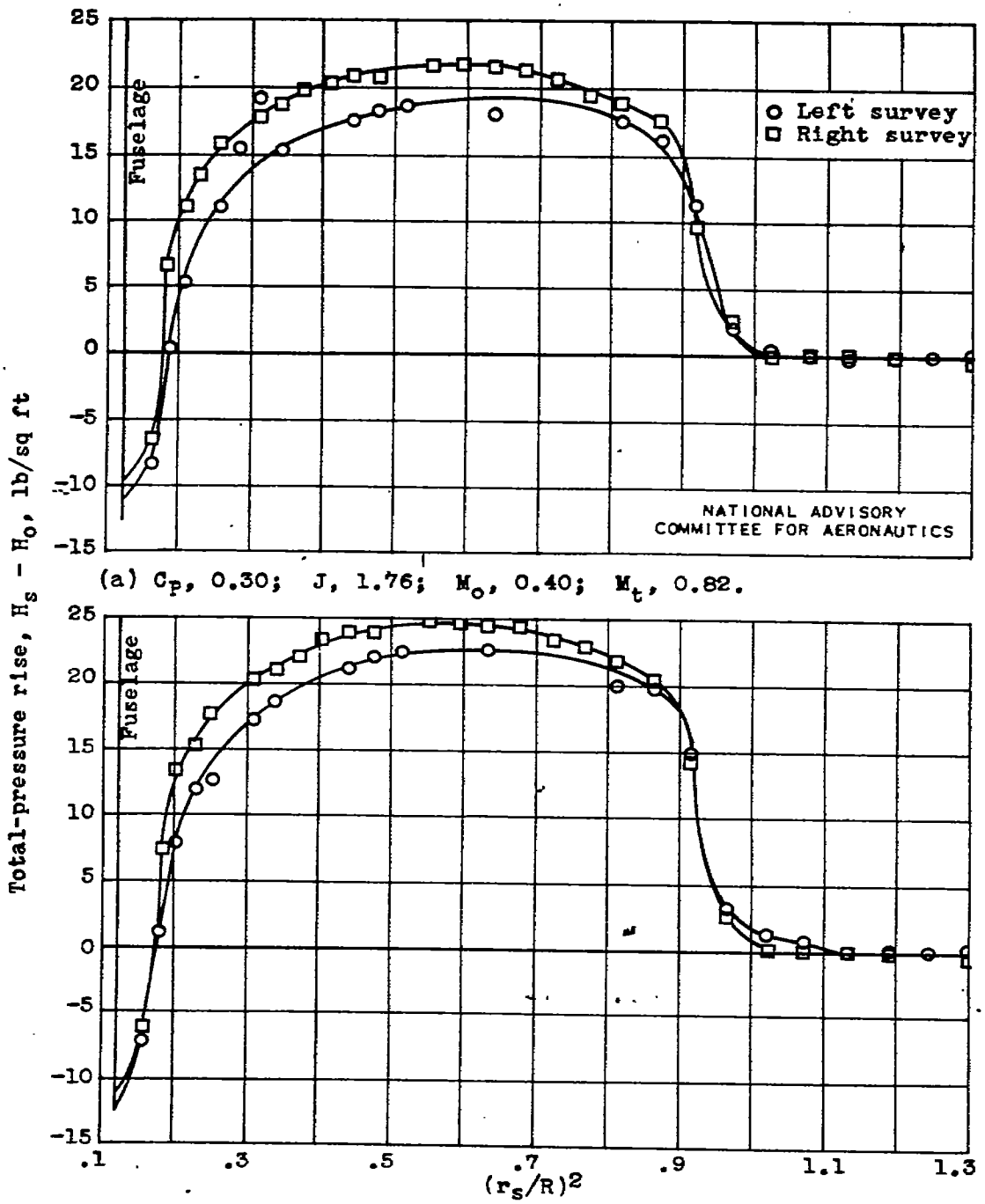

(a) C_p, 0.30; J, 1.76; M_o, 0.40; M_t, 0.82.

(b) C_p, 0.40; J, 1.85; M_o, 0.41; M_t, 0.80.

Figure 7.- Effect of power coefficient C_p on blade thrust load distribution at advance-diameter ratio J of approximately 1.75 and free-stream Mach number M_o of approximately 0.40. Aeroproducts H20C-162-X11M2 four-blade propeller.

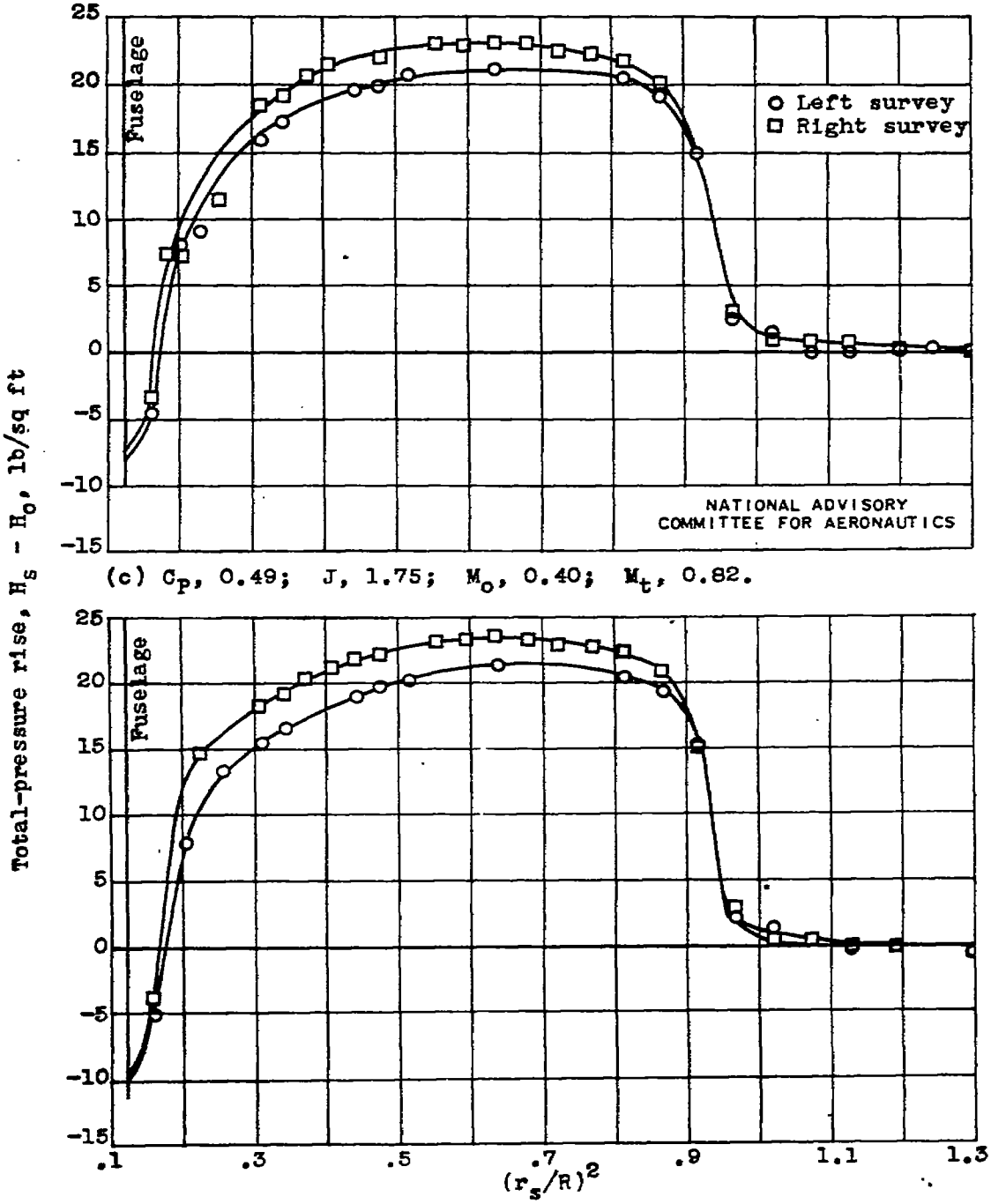

(c) C_p, 0.49; J, 1.75; M_o, 0.40; M_t, 0.82.

(d) C_p, 0.59; J, 1.83; M_o, 0.40; M_t, 0.80.

Figure 7.- Continued. Effect of power coefficient C_p on blade thrust load distribution at advance-diameter ratio J of approximately 1.75 and free-stream Mach number M_o of approximately 0.40. Aeroproducts H20C-162-X11M2 four-blade propeller.

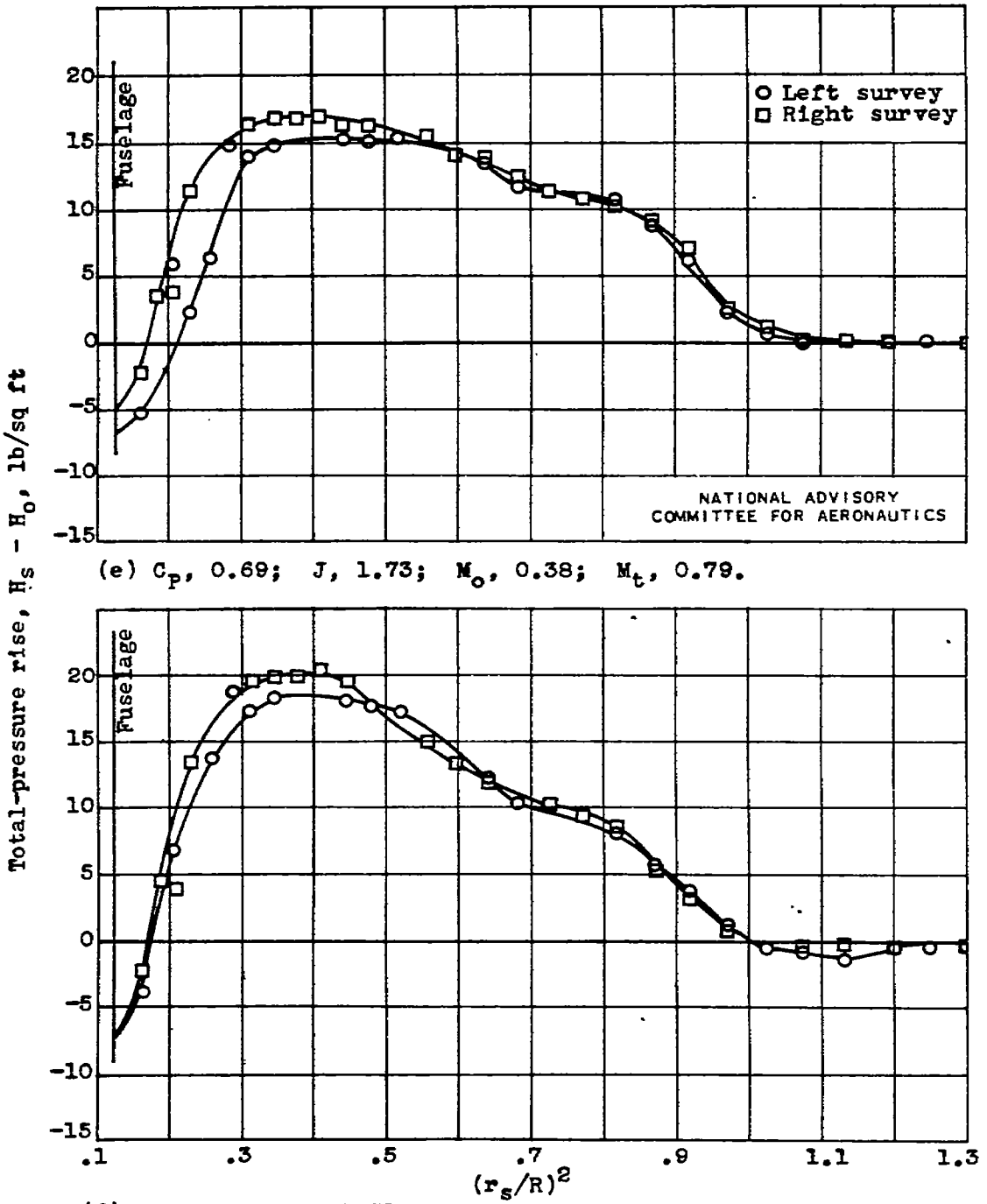

(e) C_p, 0.69; J, 1.73; M_o, 0.38; M_t, 0.79.

(f) C_p, 0.78; J, 1.71; M_o, 0.38; M_t, 0.79.

Figure 7.- Continued. Effect of power coefficient C_p on blade thrust load distribution at advance-diameter ratio J of approximately 1.75 and free-stream Mach number M_o of approximately 0.40. Aeroproducts H20C-162-X11M2 four-blade propeller.

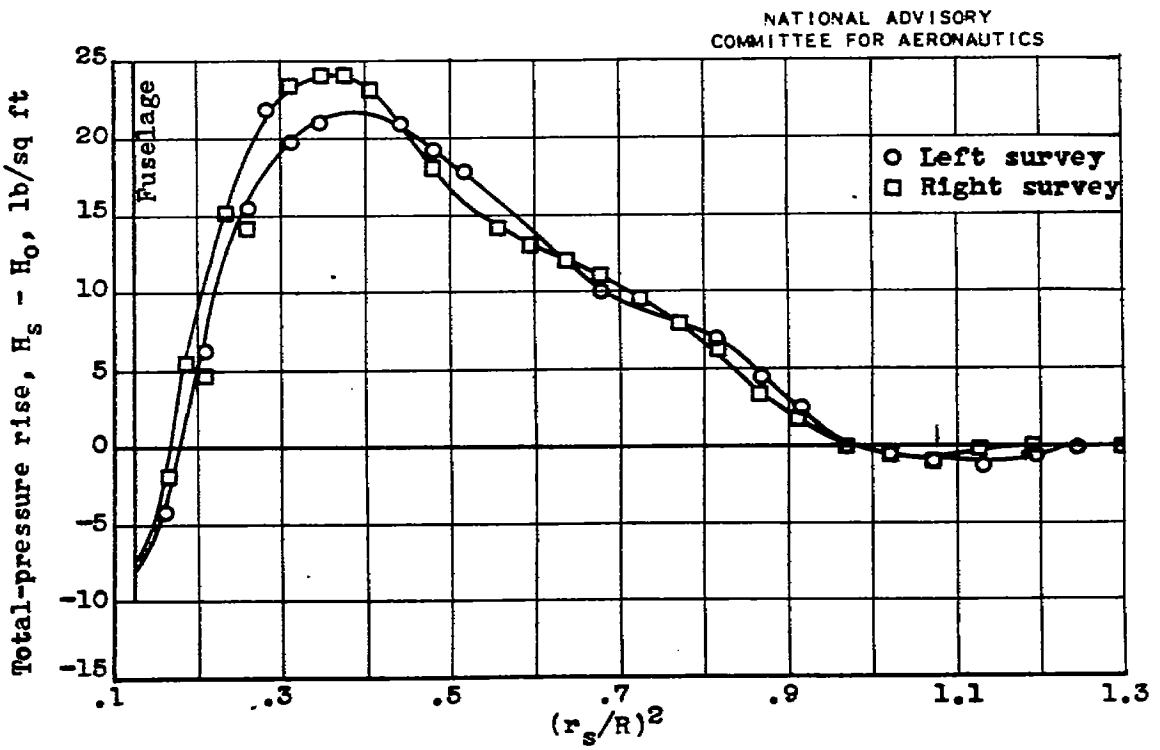

(g) C_p, 0.90; J, 1.78; M_o, 0.39; M_t, 0.79.

Figure 7.- Concluded. Effect of power coefficient C_p on blade thrust load distribution at advance-diameter ratio J of approximately 1.75 and free-stream Mach number M_o of approximately 0.40. Aeroproducts H20C-162-X11M2 four-blade propeller.

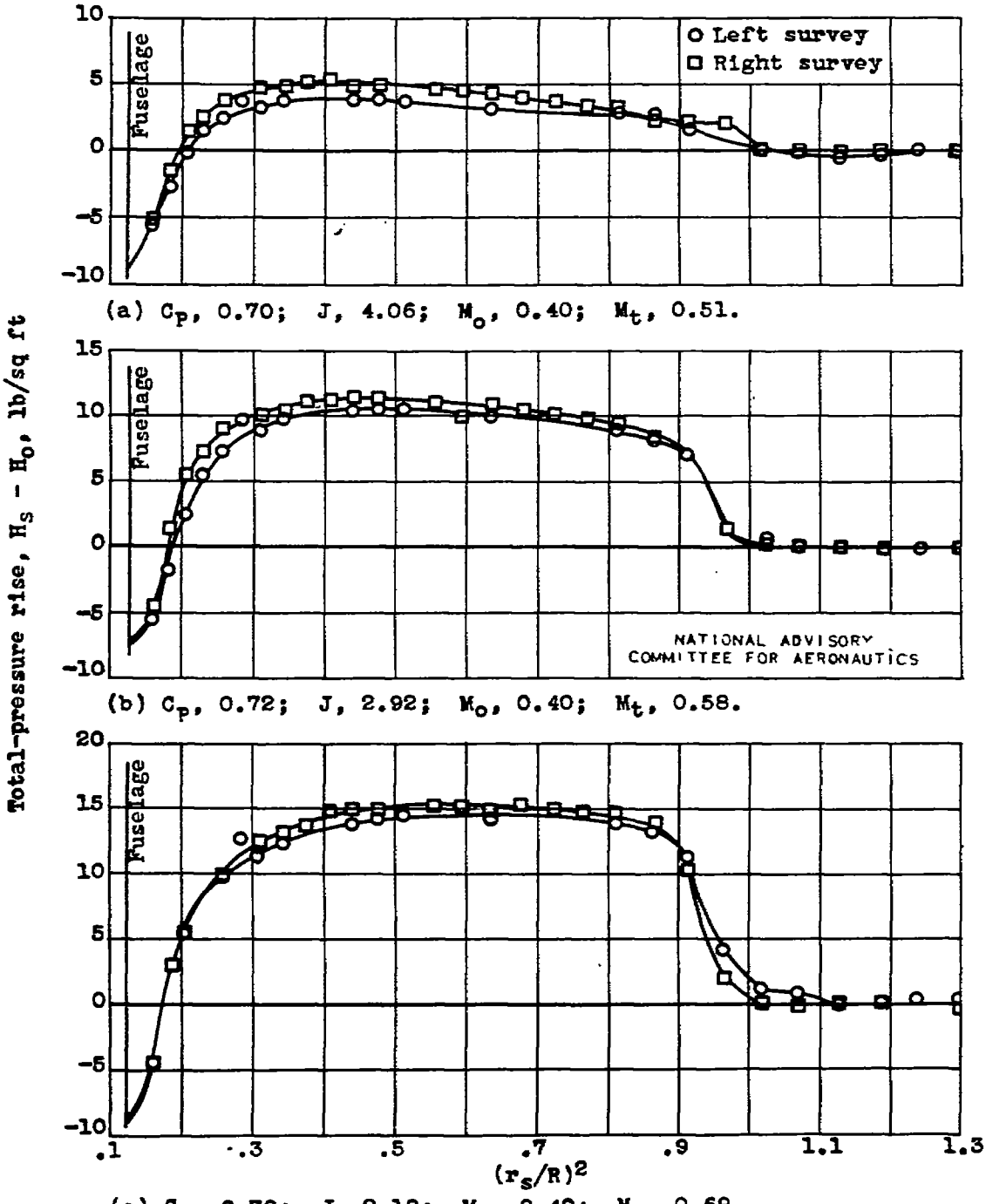

(a) C_p, 0.70; J, 4.06; M_o, 0.40; M_t, 0.51.

(b) C_p, 0.72; J, 2.92; M_o, 0.40; M_t, 0.58.

(c) C_p, 0.70; J, 2.19; M_o, 0.40; M_t, 0.69.

Figure 8.- Effect of advance-diameter ratio J on blade thrust load distribution at power coefficient C_p of approximately 0.70 and free-stream Mach number M_o of approximately 0.40. Aeroproducts H20C-162-X11M2 four-blade propeller.

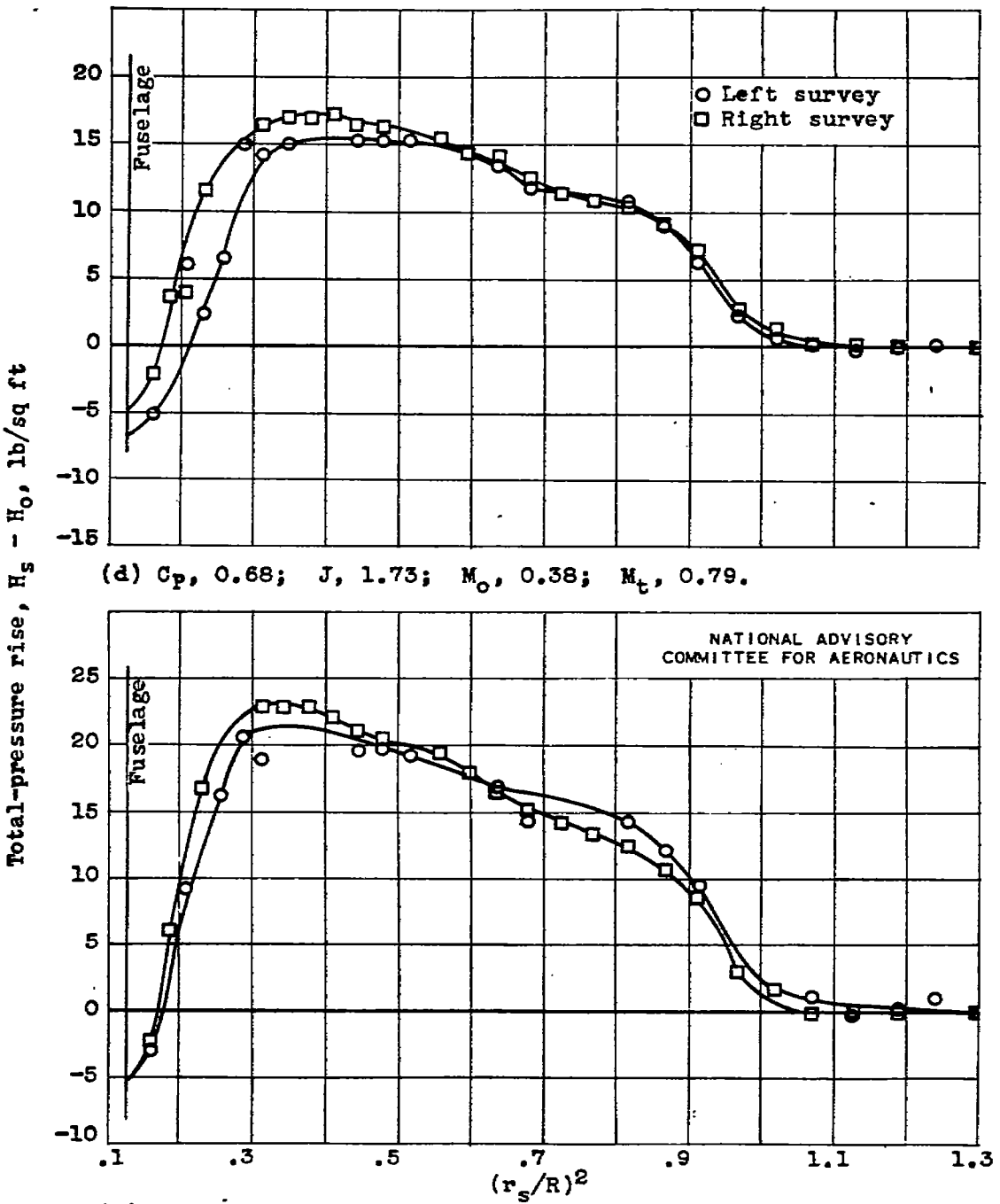

(d) C_p, 0.68; J, 1.73; M_o, 0.38; M_t, 0.79.

(e) C_p, 0.70; J, 1.58; M_o, 0.39; M_t, 0.87.

Figure 8.- Concluded. Effect of advance-diameter ratio J on blade thrust load distribution at power coefficient C_p of approximately 0.70 and free-stream Mach number M_o of approximately 0.40. Aeroproducts H20C-162-X11M2 four-blade propeller.

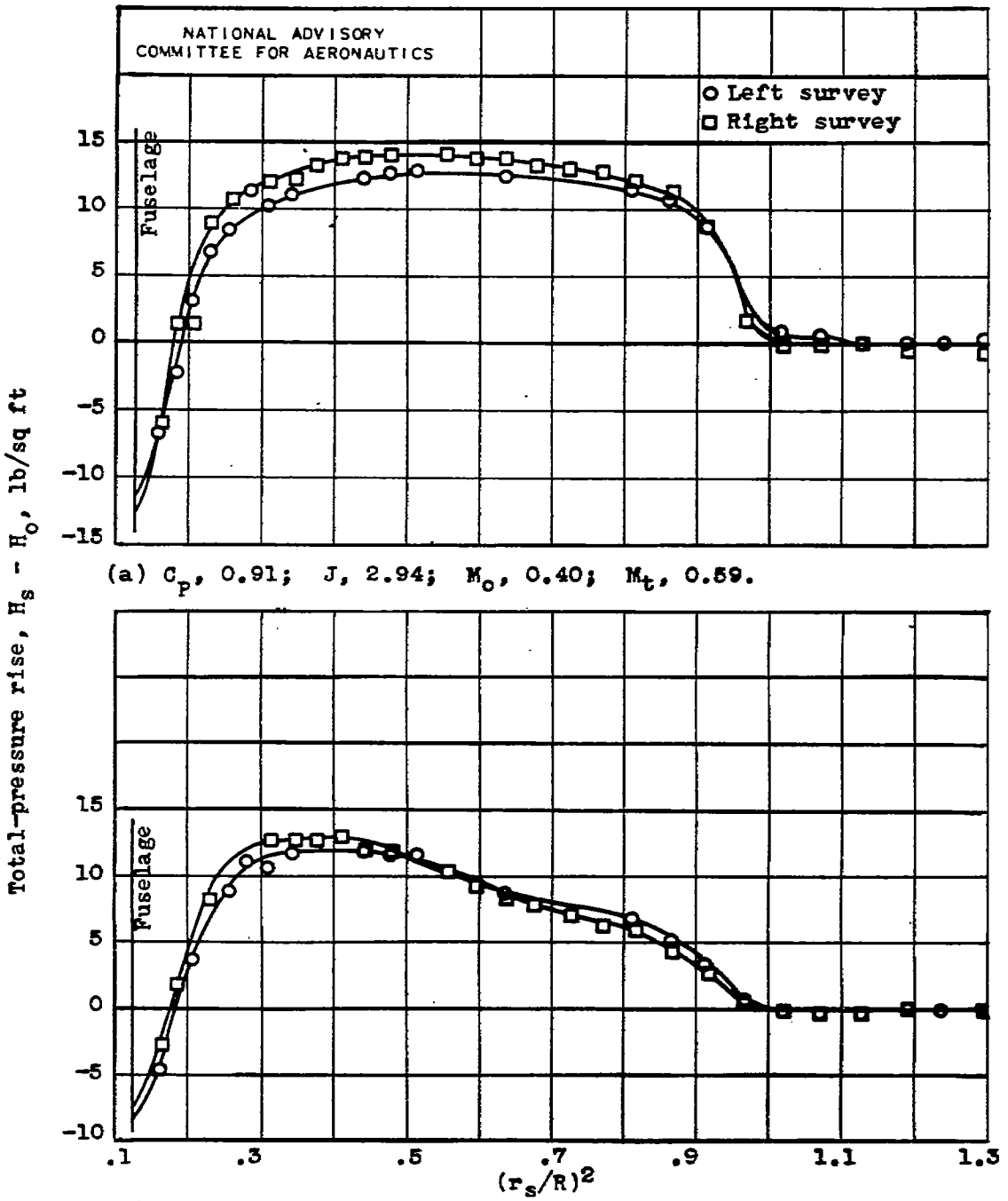

Figure 9.- Effect of advance-diameter ratio J on blade thrust load distribution at power coefficient C_p of approximately 0.90 and free-stream Mach number M_o of approximately 0.40. Aeroproducts H20C-162-X11M2 four-blade propeller.

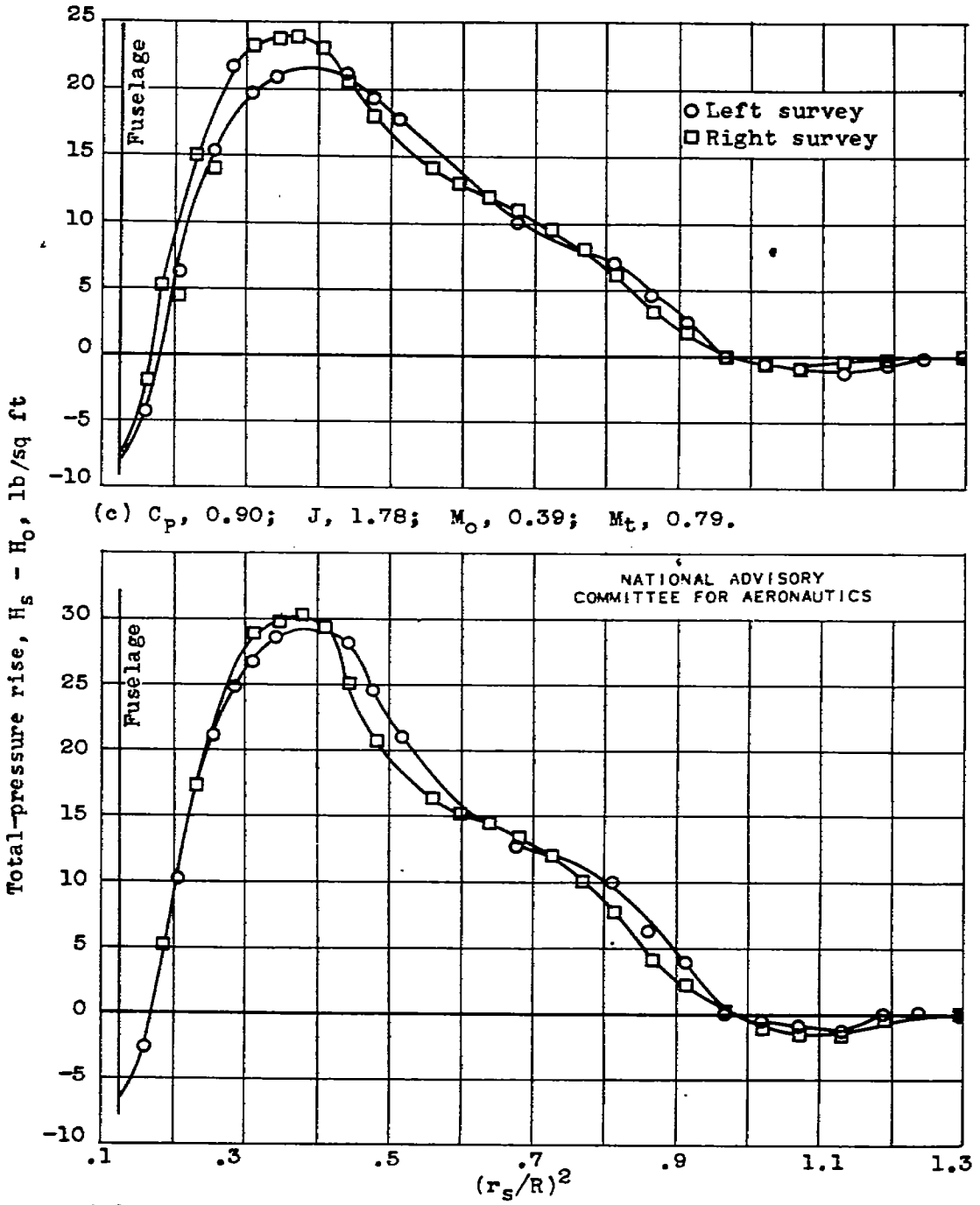

Figure 9.- Concluded. Effect of advance-diameter ratio J on blade thrust load distribution at power coefficient C_p of approximately 0.90 and free-stream Mach number M_o of approximately 0.40. Aeroproducts H20C-162-X11M2 four-blade propeller.

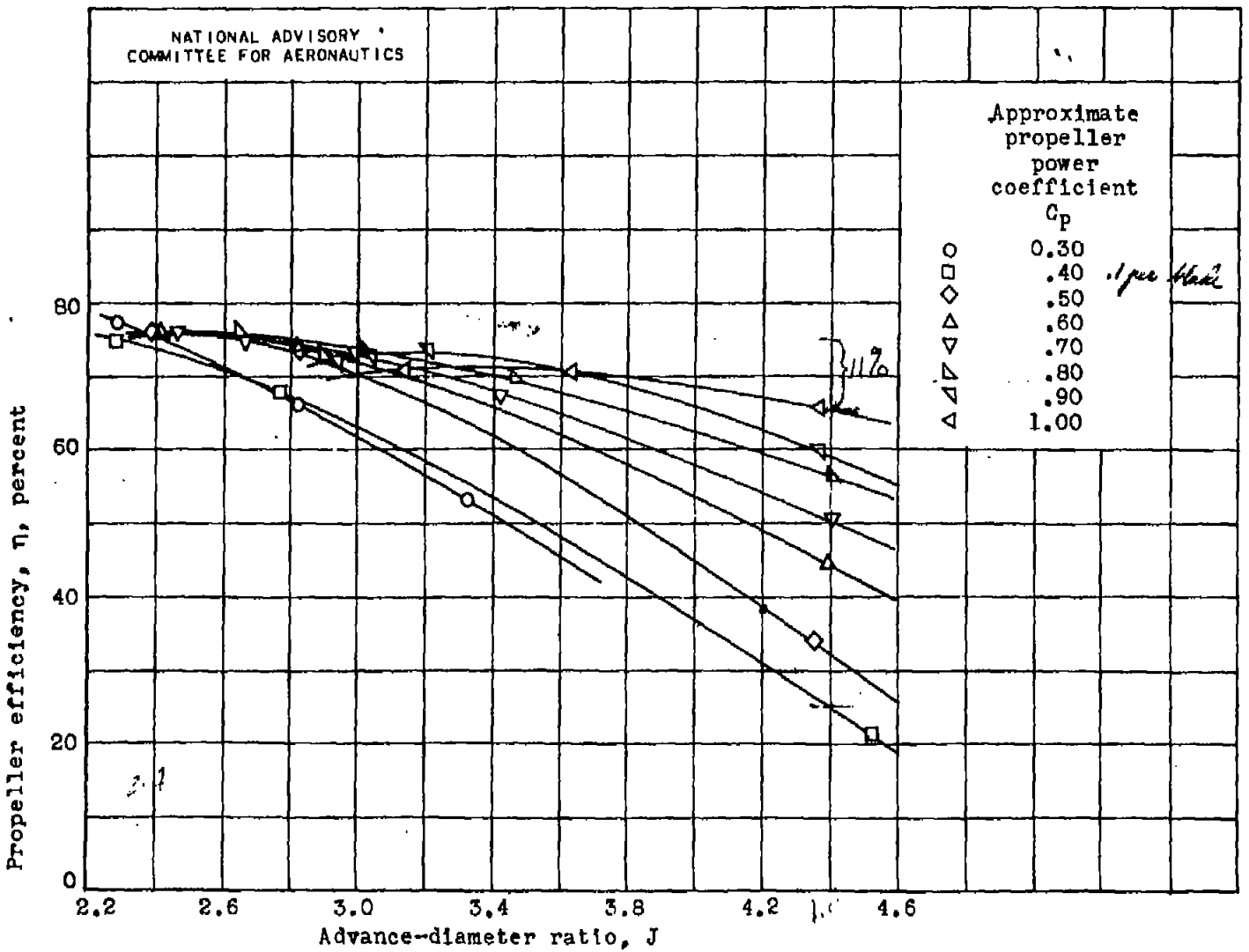

Figure 10.- Characteristics of Aeroproducts H20C-162-X11M2 four-blade propeller on YP-47M airplane at approximate free-stream Mach number M_0 of 0.50.

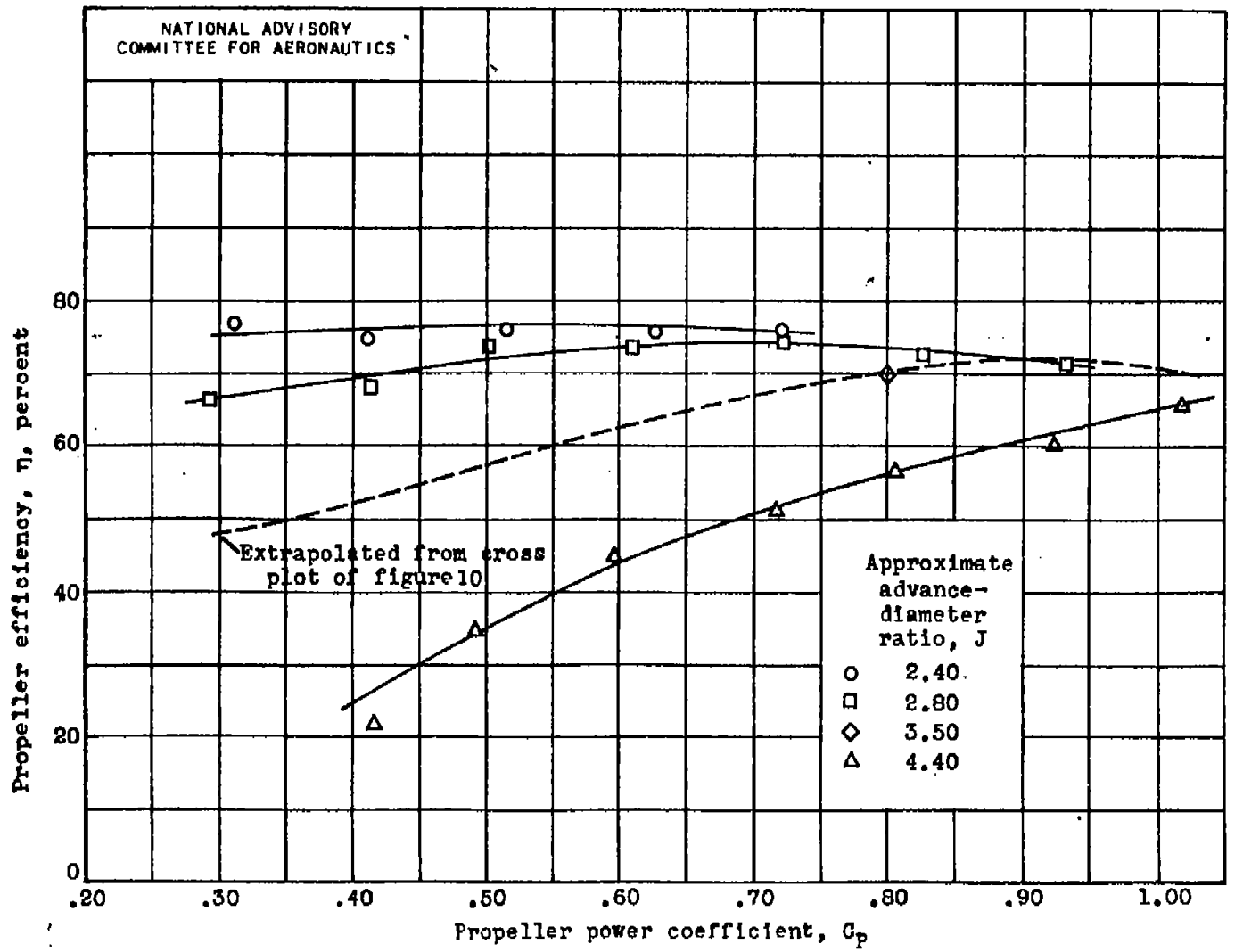

Figure 11.- Effect of power coefficient C_p on efficiency η of Aeroproducts H20C-162-X11M2 four-blade propeller at approximate free-stream Mach number M_o of 0.50.

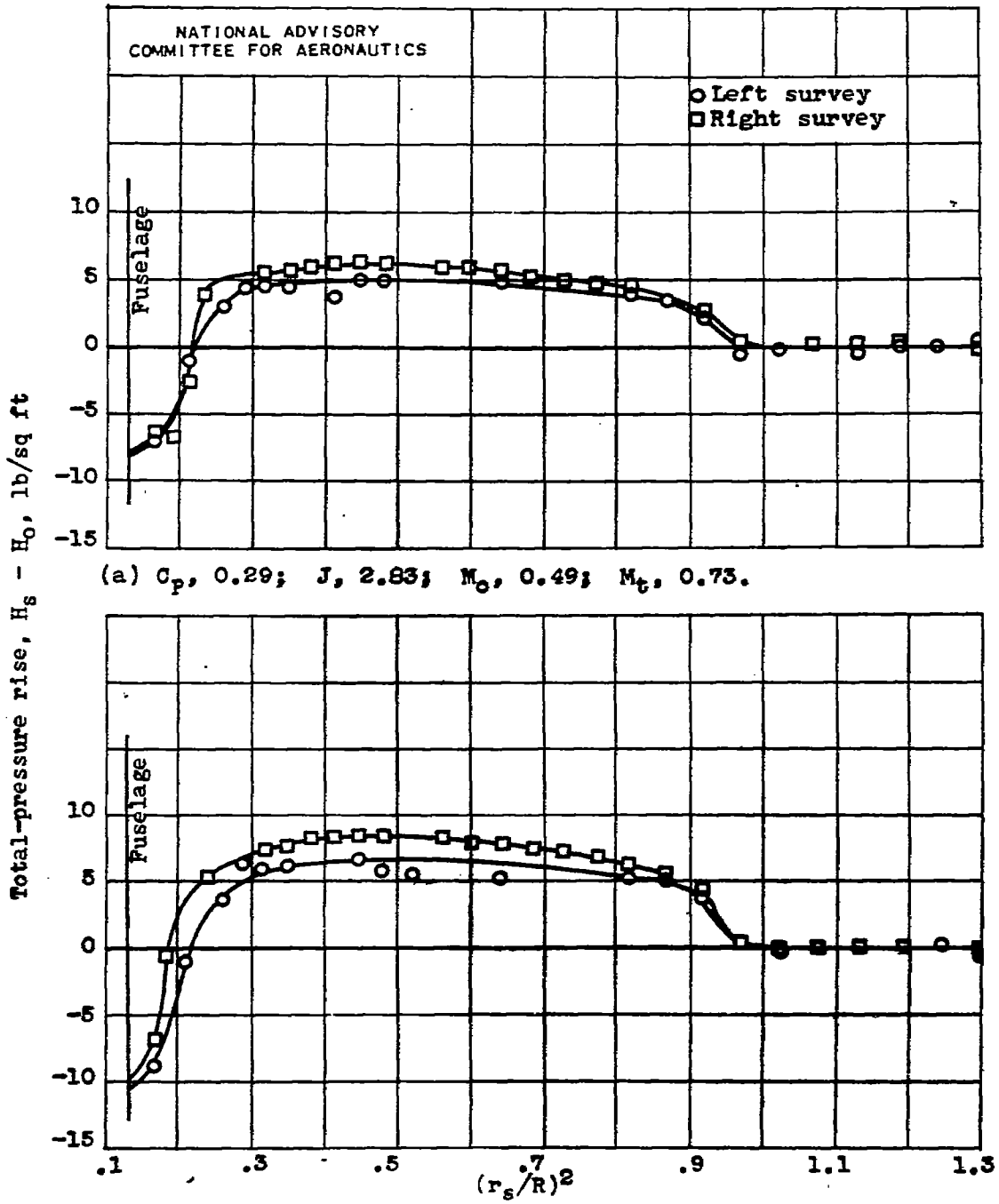

(a) C_p, 0.29; J, 2.83; M_o, 0.49; M_t, 0.73.

(b) C_p, 0.41; J, 2.78; M_o, 0.48; M_t, 0.73.

Figure 12.- Effect of power coefficient C_p on blade thrust load distribution at advance-diameter ratio J of approximately 2.80 and free-stream Mach number M_o of approximately 0.50. Aeroproducts H20C-162-X11M2 four-blade propeller.

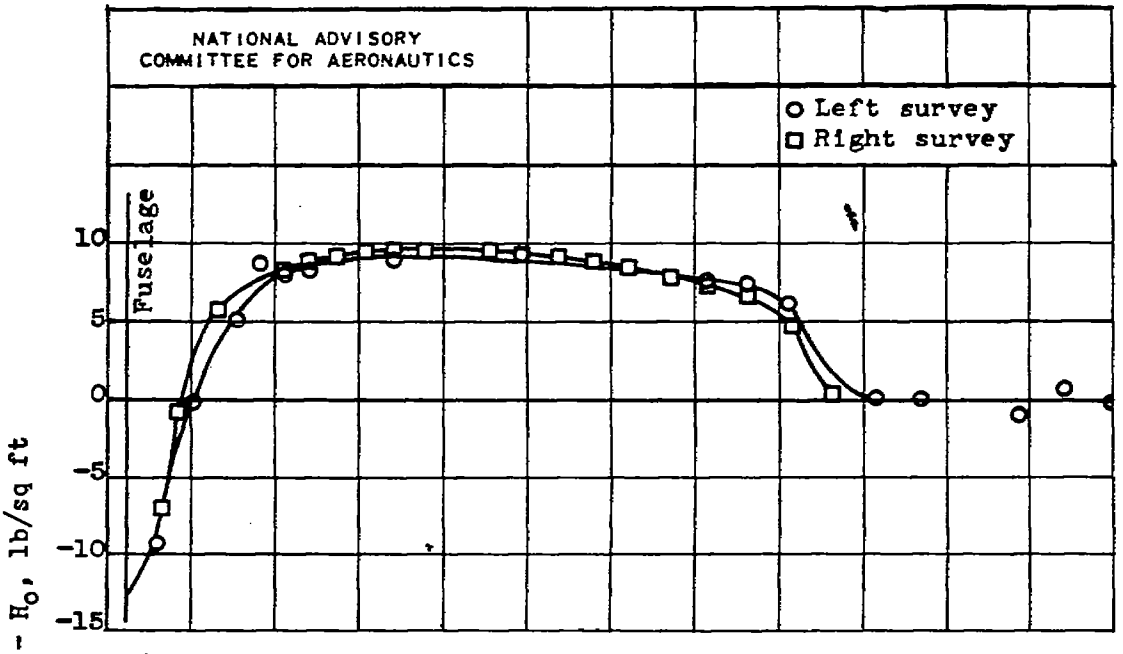

(c) C_p, 0.50; J, 2.84; M_o, 0.49; M_t, 0.74.

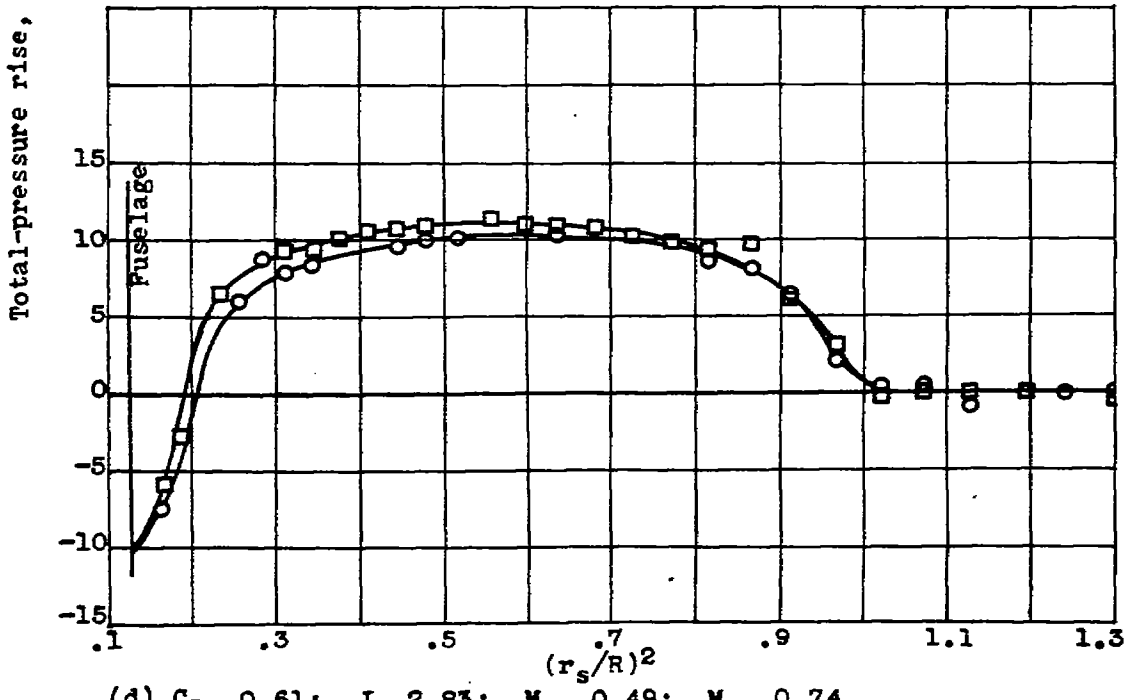

(d) C_p, 0.61; J, 2.83; M_o, 0.49; M_t, 0.74.

Figure 12.- Continued. Effect of power coefficient C_p on blade thrust load distribution at advance-diameter ratio J of approximately 2.80 and free-stream Mach number M_o of approximately 0.50. Aeroproducts H20C-162-X11M2 four-blade propeller.

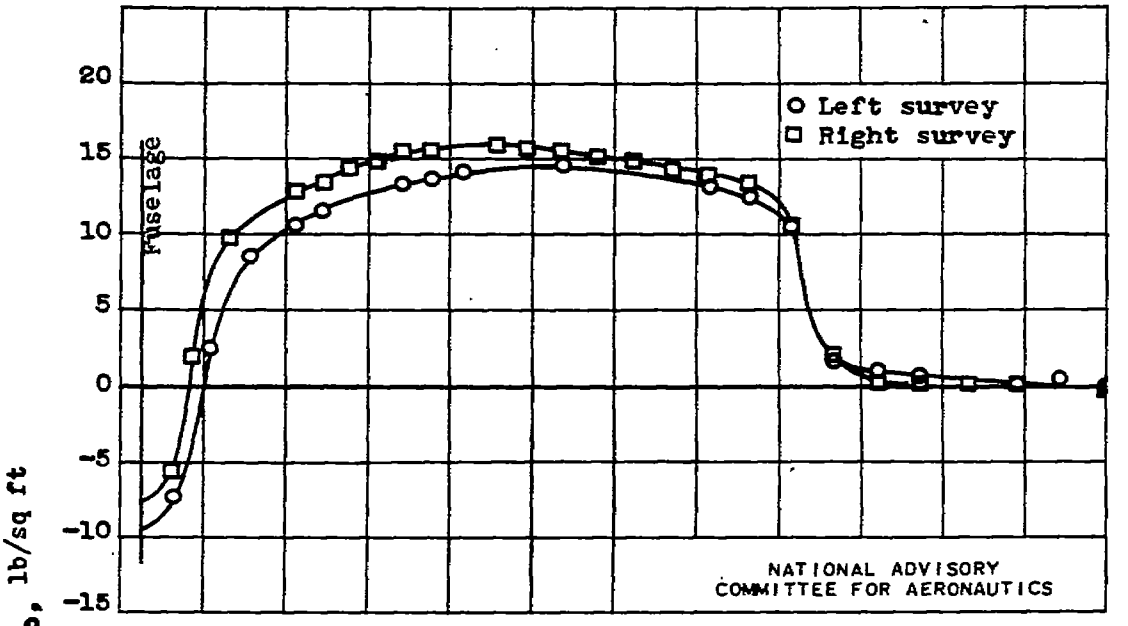

(e) C_p, 0.72; J, 2.67; M_o, 0.50; M_t, 0.77.

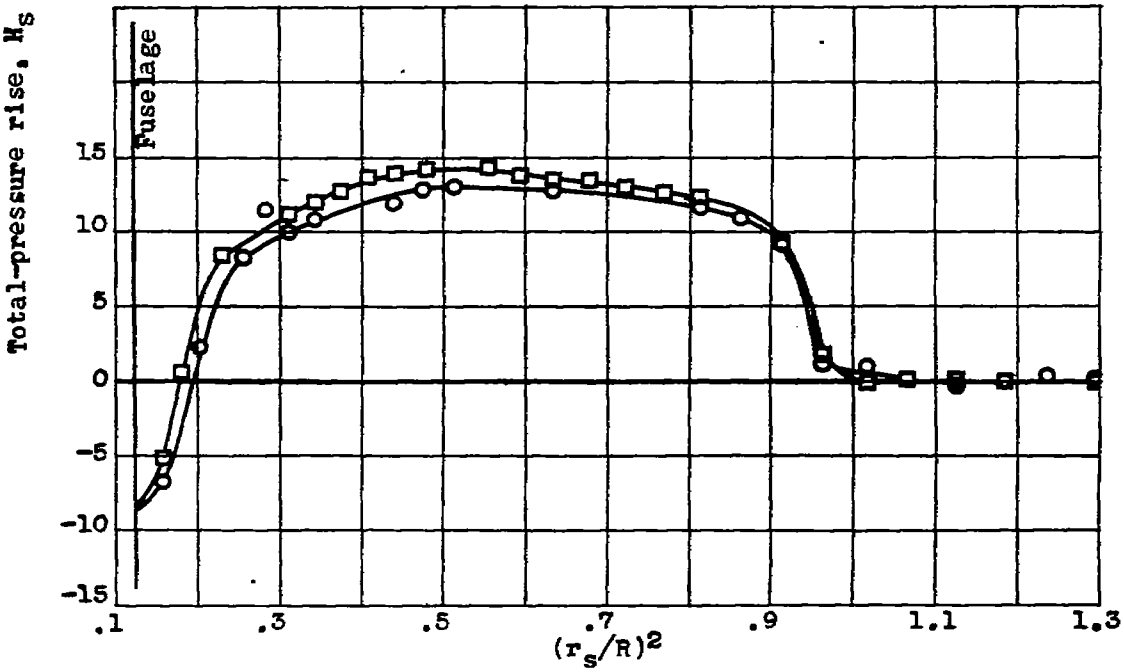

(f) C_p, 0.83; J, 2.90; M_o, 0.50; M_t, 0.73.

Figure 12.- Concluded. Effect of power coefficient C_p on blade thrust load distribution at advance-diameter ratio J of approximately 2.80 and free-stream Mach number M_o of approximately 0.50. Aeroproducts H20C-162-X11M2 four-blade propeller.

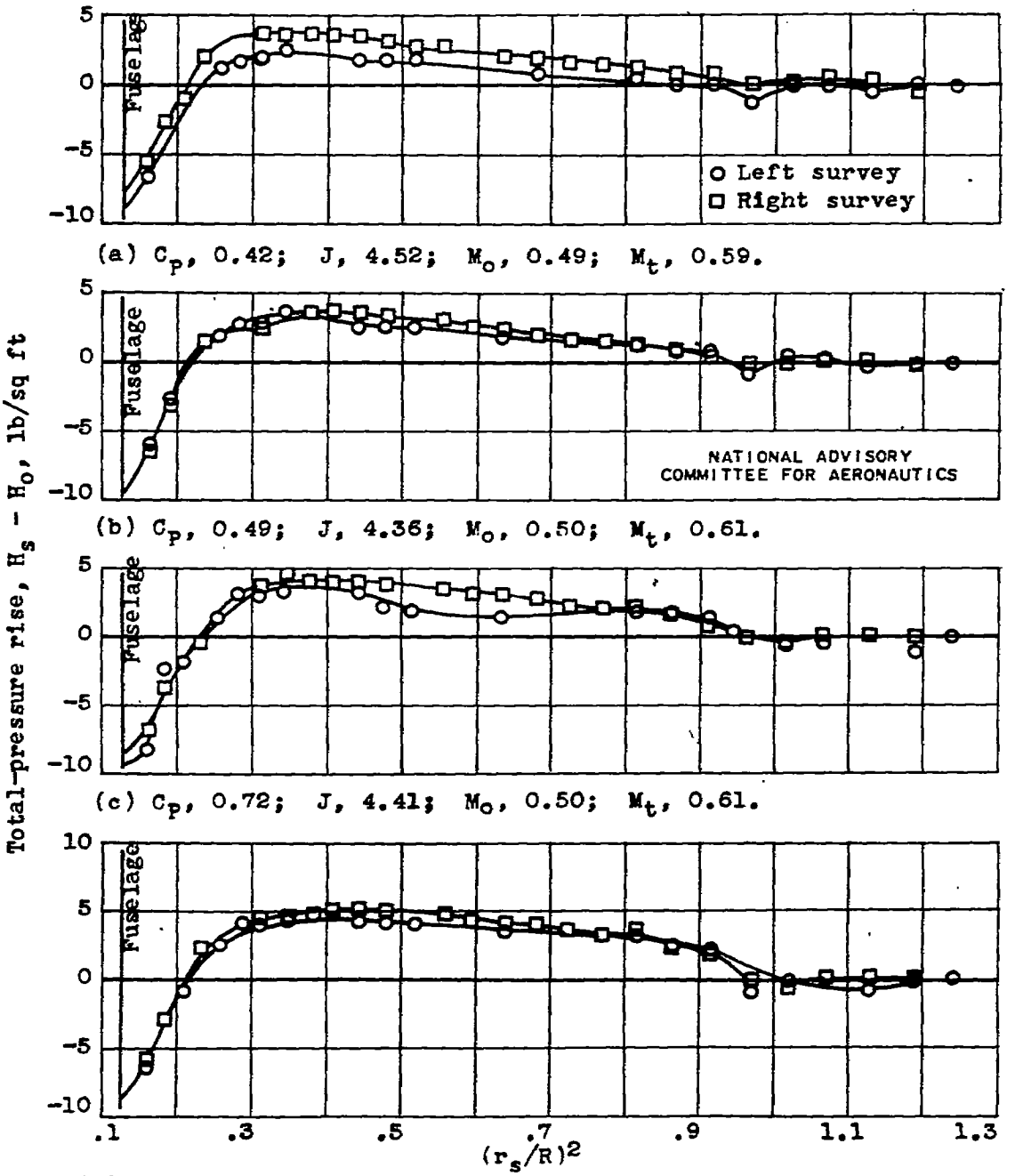

(a) C_p, 0.42; J, 4.52; M_o, 0.49; M_t, 0.59.

(b) C_p, 0.49; J, 4.36; M_o, 0.50; M_t, 0.61.

(c) C_p, 0.72; J, 4.41; M_o, 0.50; M_t, 0.61.

(d) C_p, 0.93; J, 4.36; M_o, 0.49; M_t, 0.61.

Figure 13.- Effect of power coefficient C_p on blade thrust load distribution at advance-diameter ratio J of approximately 4.40 and free-stream Mach number M_o of approximately 0.50. Aeroproducts H20C-162-X11M2 four-blade propeller.

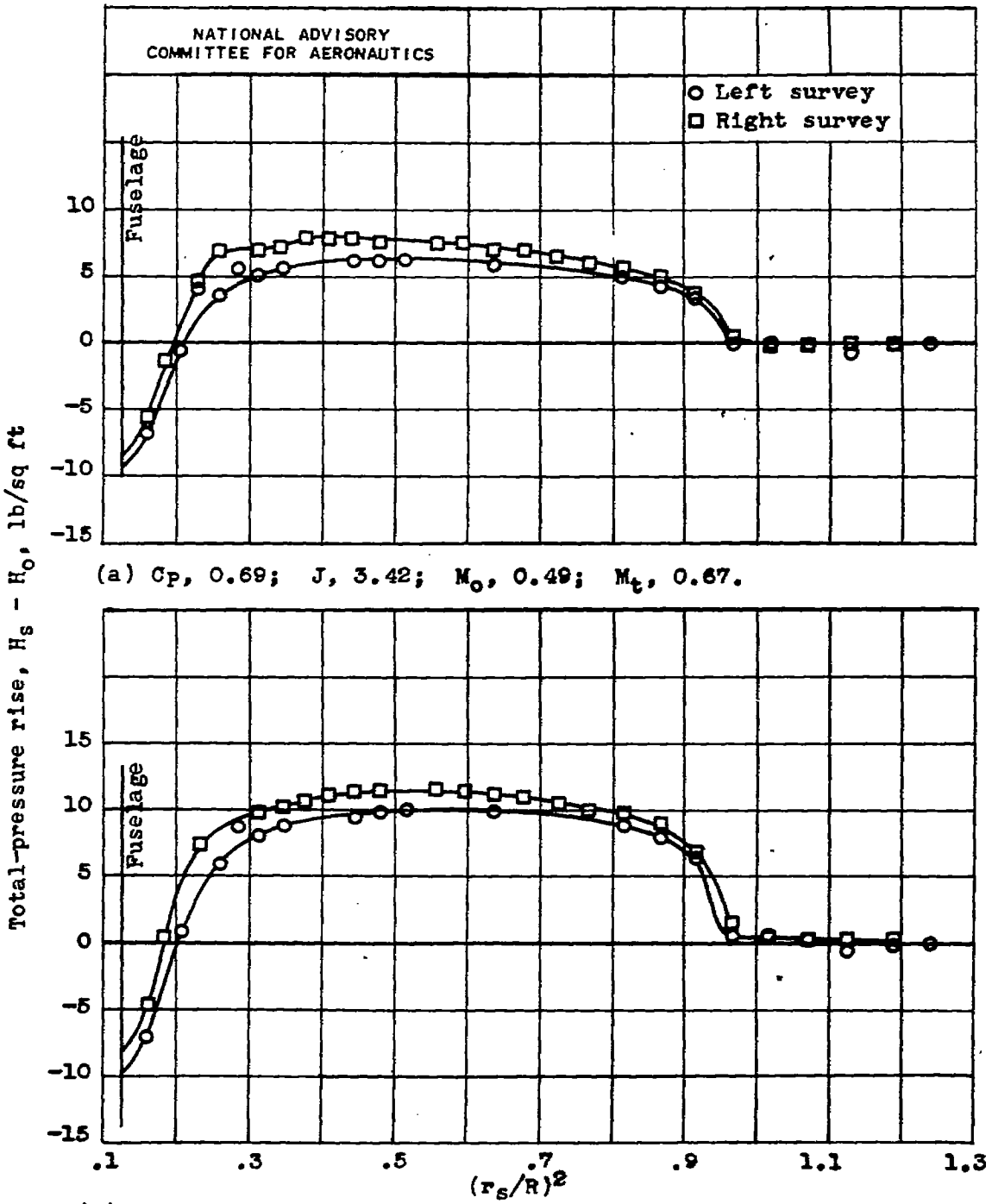

(a) C_p, 0.69; J, 3.42; M_o, 0.49; M_t, 0.67.

(b) C_p, 0.70; J, 3.01; M_o, 0.49; M_t, 0.71.

Figure 14.- Effect of advance-diameter ratio J on blade thrust load distribution at power coefficient C_p of approximately 0.70 and free-stream Mach number M_o of approximately 0.50. Aeroproducts H20C-162-X11M2 four-blade propeller.

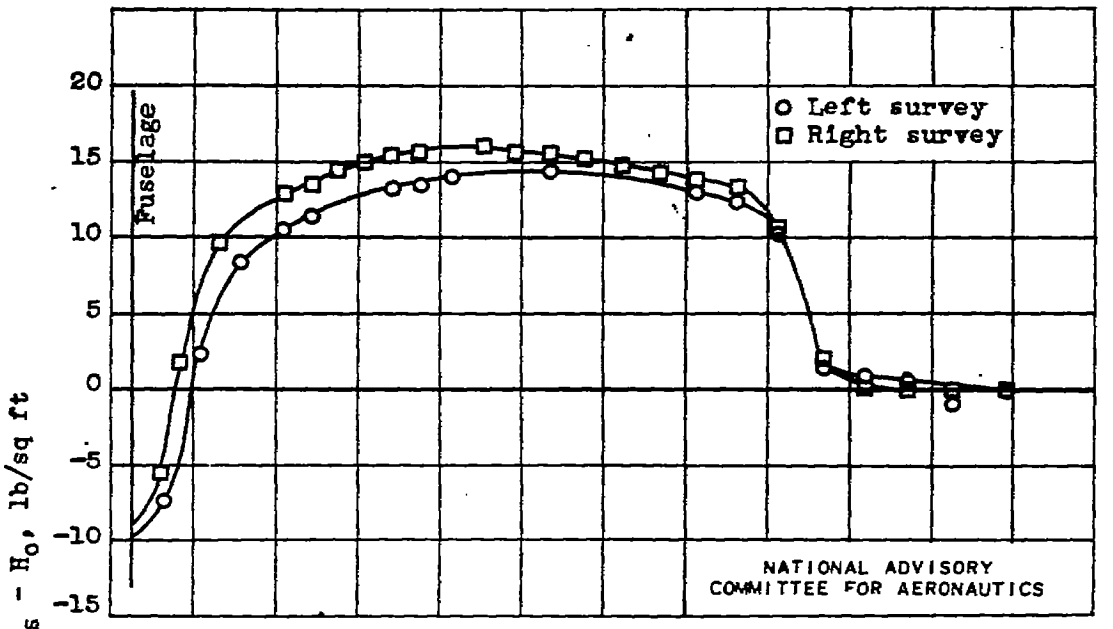

(c) C_p, 0.72; J, 2.67; M_o, 0.50; M_t, 0.77.

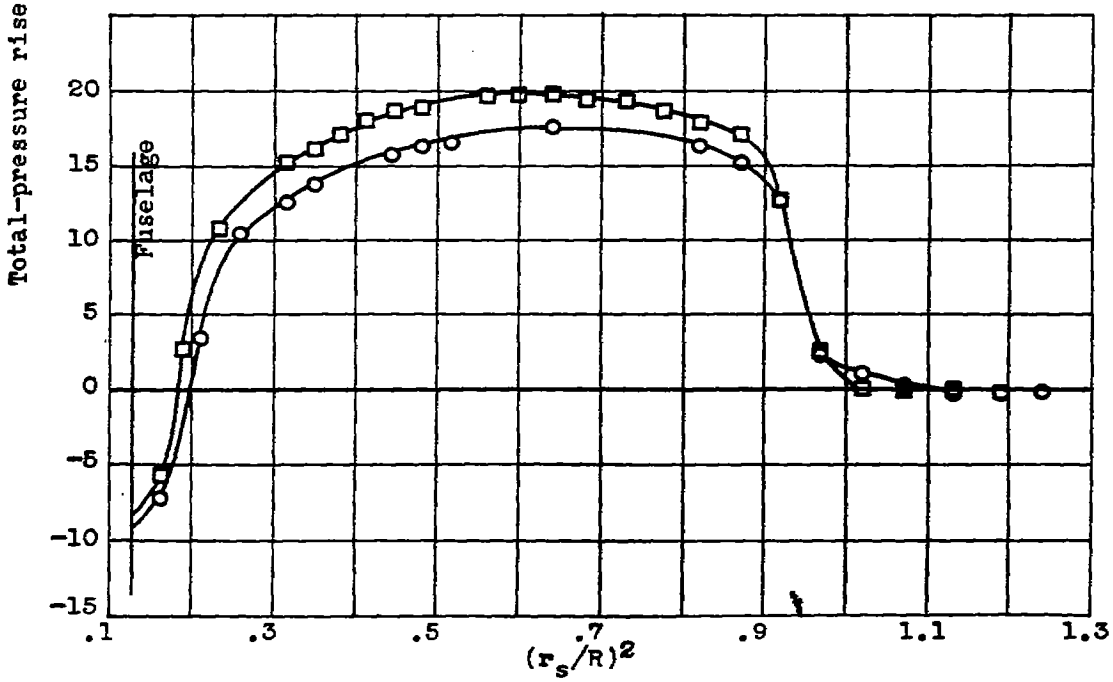

(d) C_p, 0.72; J, 2.48; M_o, 0.50; M_t, 0.81.

Figure 14.- Concluded. Effect of advance-diameter ratio J on blade thrust load distribution at power coefficient C_p of approximately 0.70 and free-stream Mach number M_o of approximately 0.50. Aeroproducts H20C-162-X11M2 four-blade propeller.

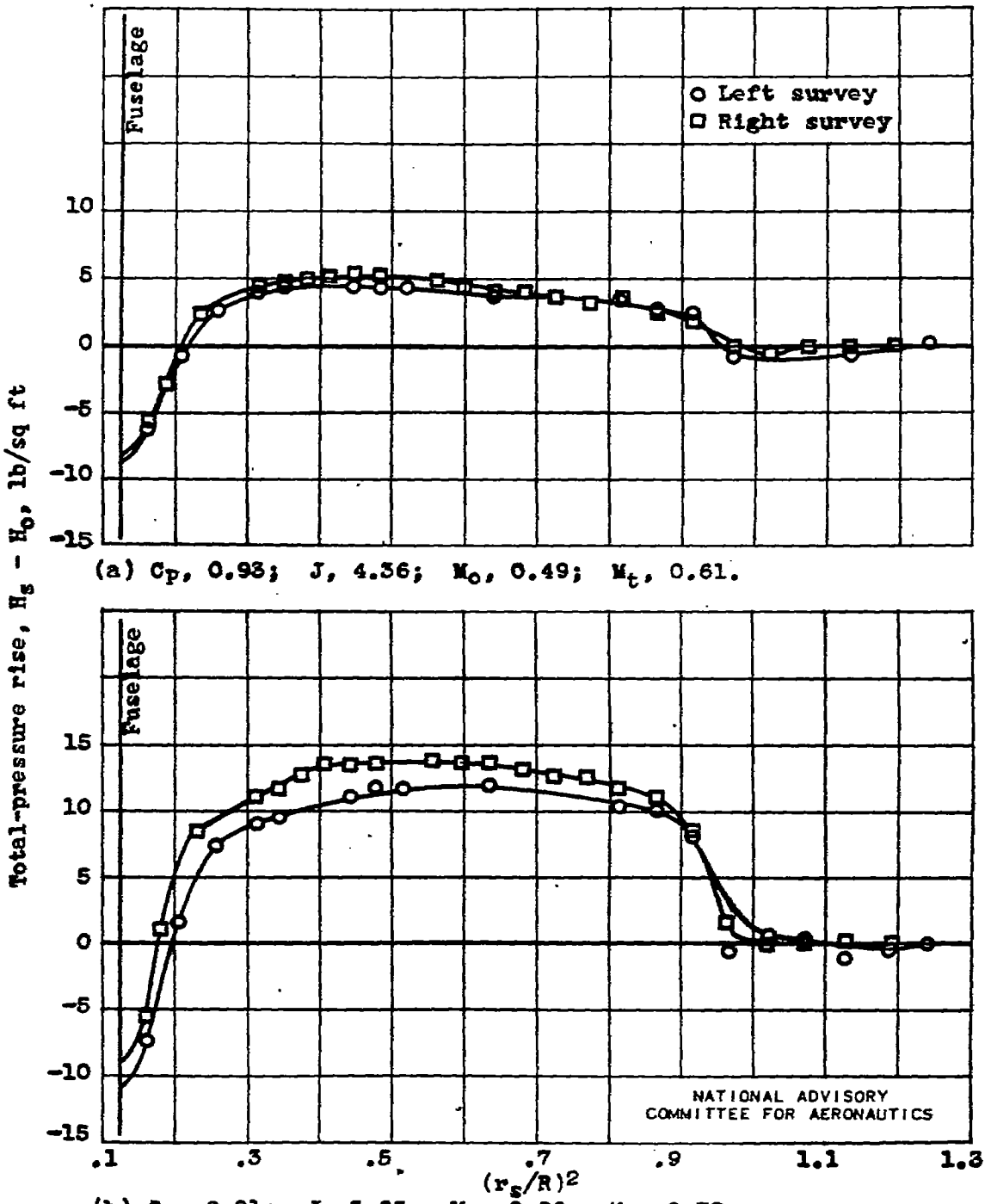

(a) C_p, 0.93; J, 4.36; M_o, 0.49; M_t, 0.61.

(b) C_p, 0.91; J, 3.05; M_o, 0.50; M_t, 0.72.

Figure 15.- Effect of advance-diameter ratio J on blade thrust load distribution at power coefficient C_p of approximately 0.91 and free-stream Mach number M_o of approximately 0.50. Aeroproducts H20C-162-X11M2 four-blade propeller.

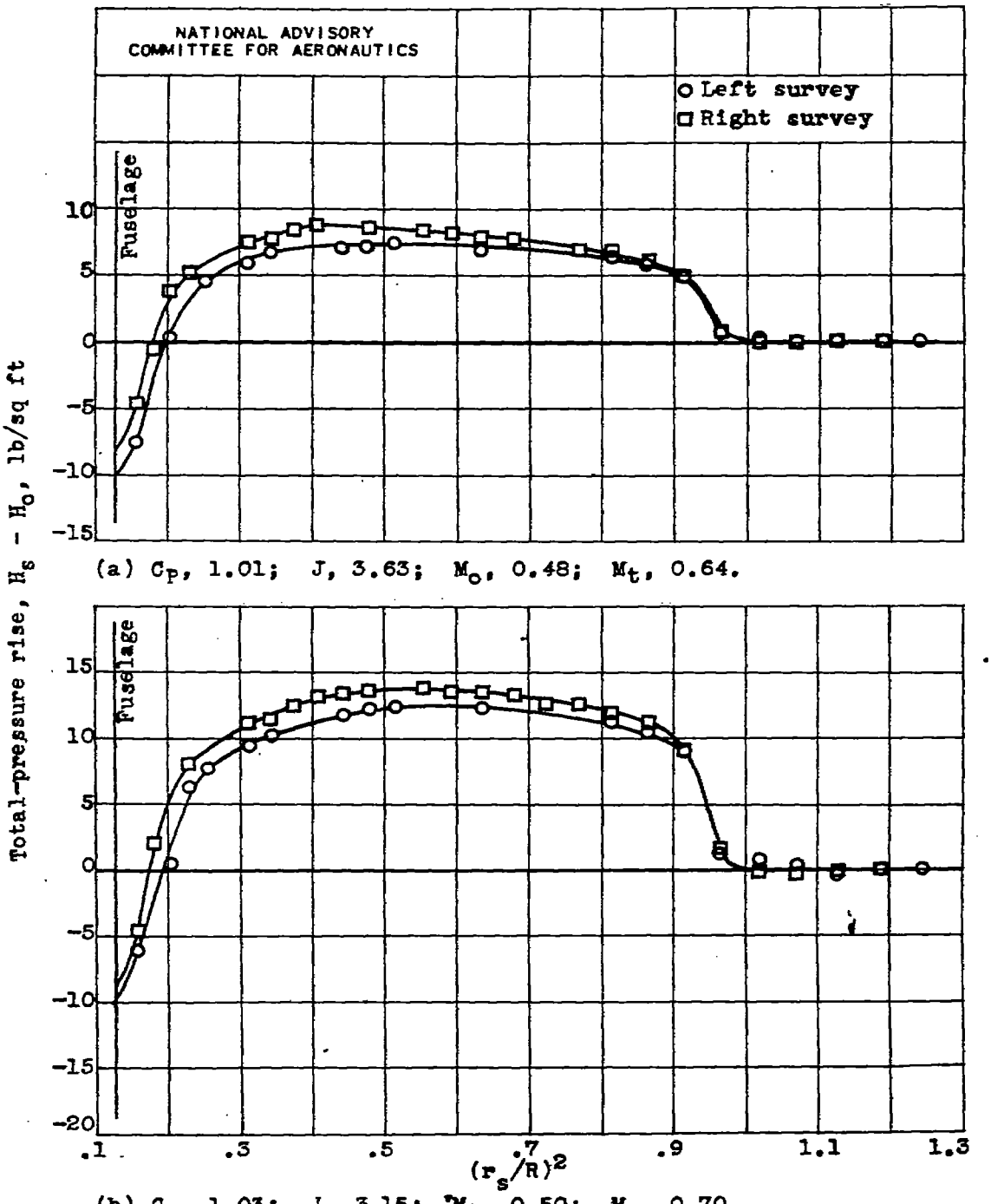

Figure 16.- Effect of advance-diameter ratio J on blade thrust load distribution at power coefficient C_p of approximately 1.00 and free-stream Mach number M_o of approximately 0.50. Aeroproducts H20C-162-X11M2 four-blade propeller.

NASA Technical Library
3 1176 01435 0285